POLITECNICO
MILANO 1863

SCUOLA DI INGEGNERIA INDUSTRIALE
E DELL'INFORMAZIONE

Hydrogen generation from different metal powders hydrolysis in aqueous solutions

Tesi di Laurea Magistrale in
Space Engineering - Ingegneria Spaziale

Author: **Silvia Antonioli**

Student ID: 975929
Advisor: Prof. Luciano Galfetti
Academic Year: 2022-2023

Abstract

The objective of this study is to explore the feasibility of utilizing the hydrolysis reaction of water with aluminum or magnesium for the purpose of generating hydrogen, which can then be utilized in various applications. Within the realm of space technology, the most significant applications include fuel cells, where it can be combined with oxygen to produce power and water, as well as space propulsion systems, such as electrical thrusters. This method of hydrogen production possesses notable benefits compared to other methods since it doesn't release CO2 or other pollutants. Aluminum is typically the preferred metal in this process due to its longevity, low toxicity, and availability at a low cost. Magnesium is also commonly employed for hydrogen production. Before the reaction can occur, it is necessary to mechanically activate the metal powders through ball milling in order to remove the protective oxide layer that forms on the metal powder upon contact with air. This layer significantly reduces the reactivity of the metal with water. To achieve mechanical activation, milling agents like $NaCl$, Bi or C are used. Once the powder is prepared, the thesis focuses on the experimental setup to assess hydrogen production for each powder formulation. Hydrogen production is evaluated using the water displacement method, where a reactor and a glass reading column filled with water are connected. The reaction takes place inside the reactor, and the resultant hydrogen moves through the connection tube to the reading column where it displaces water due to its low density, allowing for measurement of the level. Various powder formulations are tested to determine which one has the highest efficiency.

Keywords: Hydrogen generation, Mechanical activation, Aluminum powder, Magnesium powder,Water hydrolysis

Abstract in lingua italiana

L'obiettivo di questa tesi è di esplorare la fattibilità dell'utilizzo della reazione di idrolisi dell'acqua con alluminio o magnesio allo scopo di generare idrogeno, che può poi essere utilizzato in diverse applicazioni. Nel campo della tecnologia spaziale, le applicazioni più significative includono celle a combustibile, dove può essere combinato con ossigeno per produrre energia e acqua, nonché sistemi di propulsione spaziali, come i propulsori elettrici. Questo metodo di produzione di idrogeno possiede notevoli vantaggi rispetto ad altri metodi poiché non rilascia CO2 o altri inquinanti. L'alluminio è tipicamente il metallo preferito in questo processo a causa della sua longevità, bassa tossicità e disponibilità a basso costo. Il magnesio è anche comunemente impiegato per la produzione di idrogeno. Prima che la reazione possa avvenire, è necessario attivare meccanicamente le polveri metalliche attraverso la frantumazione a sfere al fine di rimuovere lo strato di ossido protettivo che si forma sulla polvere metallica a contatto con l'aria. Questo strato riduce significativamente la reattività del metallo con l'acqua. Per ottenere l'attivazione meccanica, vengono utilizzate diverse sostanze come $NaCl$, Bi o C. Una volta preparata la polvere, la tesi si concentra sulla configurazione sperimentale per valutare la produzione di idrogeno per ciascuna formulazione. La produzione di idrogeno viene valutata utilizzando lo spostamento dell'acqua, dove un reattore e un cilindro graduato in vetro riempiti d'acqua sono connessi. La reazione avviene all'interno del reattore e l'idrogeno prodotto si muove attraverso il tubo di connessione verso la colonna di lettura dove a causa della sua bassa densità, sposta l'acqua, consentendo la misurazione del livello. Vengono testate diverse formulazioni per determinare quale ha la maggiore efficienza.

Parole chiave: Generazione di idrogeno, Attivazione meccanica, Polvere di alluminio, Polvere di magnesio, Idrolisi dell'acqua

Contents

List of Symbols

MPD Magneto Plasma Dynamics
DC Direct Current arcjet
Al Aluminum
Mg Magnesium
$NaCl$ Sodium chloride
KCl Potassium chloride
Bi Bismuth
C Graphite
Sn Tin
In Indium
Ga Gallium
Hg Mercury
Li Lithium
Zn Zinc
Fe Steel
Co Copper
Ni Nichel
CO_2 Carbon dioxide
H_2 Hydrogen
H_2O Water
M Metal
M_xO_y Metal oxide
$M(OH)_{\frac{2y}{x}}$ Metal Hydroxide
$Al(OH_3$ Aluminum hydroxide
$AlOOH$ Aluminum hydroxide oxide
Al_2O_3 Alumina
$BaCl_2$ Barium chloride
Bi_2O_3 Bismuth oxide
$Bi(OH)_3$ Bismuth hydroxide

$NaOH$ Sodium hydroxide
KOH Potassium hydroxide
$Na_2Al_2O_4$ Sodium aluminate
$Mg(OH)_2$ Magnesium hydroxide
n_{Al} Aluminum number of moles
n_{H_2} Hydrogen number of moles
m_{Al} Aluminum mass
M_{Al} Aluminum molar mass
m_{H_2} Hydrogen mass
n_{H_2} Hydrogen number of moles
M_{H_2} Hydrogen molar mass
V_{H_2} Hydrogen volume
ρ_{H_2} Hydrogen density
P_{H_2} Hydrogen pressure
R_{H_2} Hydrogen gas constant
$T_{reaction}$ Ambient temperature
P_{amb} Ambient pressure
P_{H_2O} Water pressure
A Antoine's constant
B Antoine's constant
C Antoine's constant
eff Reaction efficiency
$V_{H_{2real}}$ Real volume of produce hydrogen
$V_{H_{2stoich}}$ Stoichiemtric volume of producible hydrogen
R_u Universal gas constant 2θ XRD diffraction angle

List of Figures

List of Tables

1 | Introduction

The utilization of hydrogen as a fuel has become increasingly vital in the automotive and aerospace industries due to its low environmental impact and high energy efficiency, as well as its abundance on Earth. However, hydrogen is not yet widely used because of concerns regarding its storage and production safety. Its low density necessitates cylinders that can endure high pressure, and it is also highly flammable and explosive. To address these issues, alternative methods for producing hydrogen are being explored, such as direct production when needed. One such method is the hydrolysis reaction, which is a green reaction that does not generate harmful byproducts for the environment. Aluminum and magnesium are metals that have been studied for their potential to facilitate this reaction due to their abundance, low toxicity, and high stability. Furthermore, aluminum is often found as refuse material in numerous industries, allowing it to be repurposed for hydrogen production. Both aluminum and magnesium are used in powder form as increasing reactivity, which is necessary for the reaction, accompanies a reduction in particle size. However, these metals are not reactive when added directly to water because of the oxide layer created when exposed to air. To create a reaction, mechanical activation and additives are necessary to eliminate this protective layer and enable the metal to interact with water. The assessment of overall hydrogen production for the metal investigated is essential to comprehend the amount of hydrogen that can be produced from a single gram of the metal and provide insight into which applications would benefit from this hydrogen source.

1.1. Objectives

The primary aim of this thesis is to determine the optimal powder formulation for generating hydrogen. Various powders were experimented under identical conditions to facilitate comparisons and identify those with the highest reaction effectiveness. This research is useful for determining potential candidates for the advancement of fuel cell technology in space.

1.2. Plan of Presentation

This thesis is divided in 5 chapters organized as follows:

- **Chapter 1**: It offers a concise overview of both the research topic, the conducted experiments, and the study's objectives.
- **Chapter 2**: The discourse encompasses an evaluation of current techniques for hydrogen generation, exploring various factors that can be modified to enhance the efficiency of production.
- **Chapter 3**: The study outlines the methodology used in creating aluminum tablets and generating hydrogen, presenting findings from the experimental tests conducted. The results are thoroughly analyzed to determine the optimal formulation for hydrogen production.
- **Chapter 4**: This discusses the potential uses of hydrogen in space technology, particularly for the purpose of space propulsion.
- **Chapter 5**: Conclusion of the work and possible future developments.

2 | State of the art

The use of hydrogen is becoming increasingly important as an alternative to fossil fuels in order to reduce pollution and address the issue of their depletion. Hydrogen is a free and carbon-free source of energy with high energy density. While hydrogen can already be produced on a large scale through reforming, the raw materials used are based on fossil fuels and therefore emit CO_2. However, the production and storage of hydrogen present some challenges. Due to its low density, high pressure tanks and insulation are necessary for storage, and it can be explosive when mixed with air.

To address these issues, an in-situ production approach could be employed, whereby hydrogen is directly produced through the hydrolysis reaction of water by reacting it with a metal such as aluminum or magnesium. This reaction yields environmentally friendly products and can also be used in fuel cell applications.

2.1. Hydrogen generation through different metal powders

One can produce hydrogen on-site by reacting various metals with water. Several commonly used and environmentally stable metals, such as aluminum, magnesium, and silicon, can be utilized for this purpose. These metals possess key traits, such as safe storage and transportation, and prolonged shelf life. Additionally, the reaction yields a substantial amount of heat and results in metal oxides or hydroxides, which are chemically inactive and easy to store. Moreover, the metal oxides or hydroxides can be reprocessed into pure metals via current metal smelting processes.

By using stoichiometric equations, it is possible to calculate the theoretical quantity of hydrogen that can be generated. The reactions can be categorized based on the type of metal oxide or hydroxide produced. Here are the general equations for both scenarios.

$$xM + yH_2O \longrightarrow M_xO_y + yH_2 \tag{2.1}$$

$$xM + 2yH_2O \longrightarrow xM(OH)_{2y/x} + yH_2 \tag{2.2}$$

The following figure displays the maximum potential hydrogen output that can be achieved theoretically using each metal powder [21].

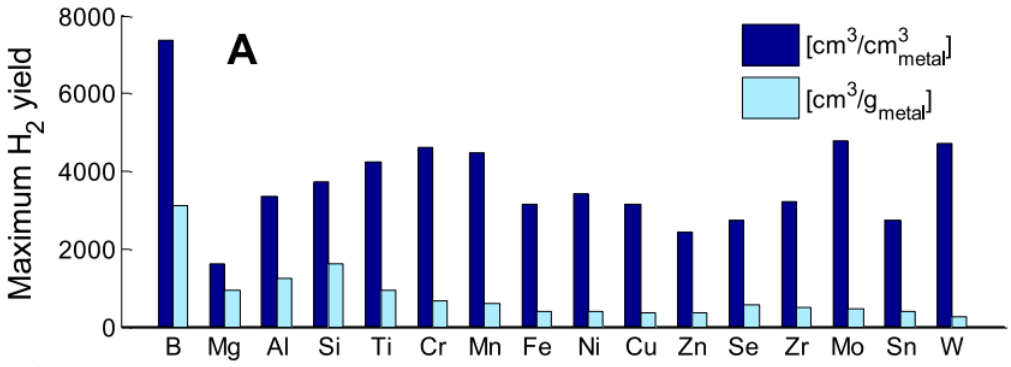

Figure 2.1: Hydrogen yield from different metal powders [21].

Based on these findings, boron appears to be the most effective metal for hydrogen generation, with aluminum, magnesium, and silicon also ranking highly due to their reactivity. In theory, heavier metals such as titanium, chromium, or manganese could also generate significant volumes of hydrogen on a volumetric basis

One of the factors investigated during the analysis of different metal powders is the overall hydrogen output. It can be observed that the powders with the highest specific energy levels, namely aluminum, magnesium, silicon, and boron, produce the greatest yield of hydrogen. Conversely, metals with low energy levels, such as copper, nickel, and selenium, produce minimal quantities of hydrogen.

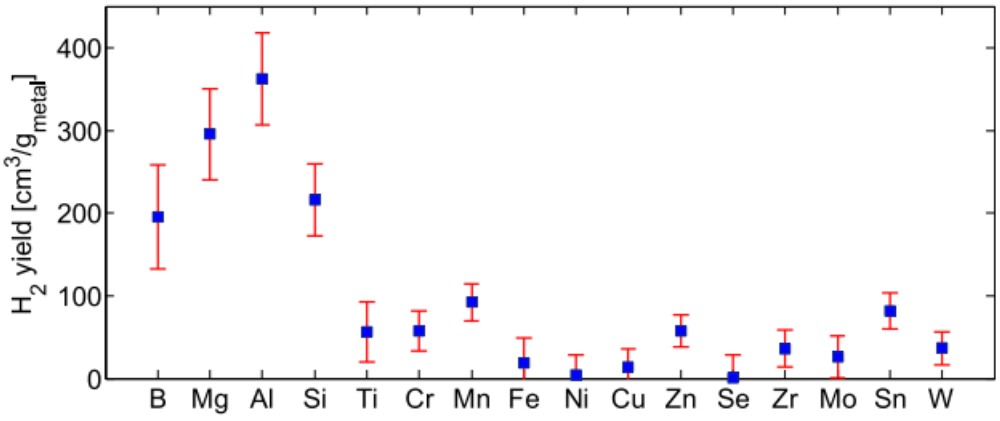

Figure 2.2: Experimental hydrogen yield from different metal powders[21].

Evaluating the reaction rate of the metal powder is a crucial aspect of research, as it plays a significant role in determining the rate of energy delivery, which is important for potential applications of the generated hydrogen in future reactors. As the reaction between the metal and water occurs mainly on the surface, the reaction rate is directly correlated with the total surface area of the sample. Based on this, aluminum and magnesium have the highest production rate per unit area.

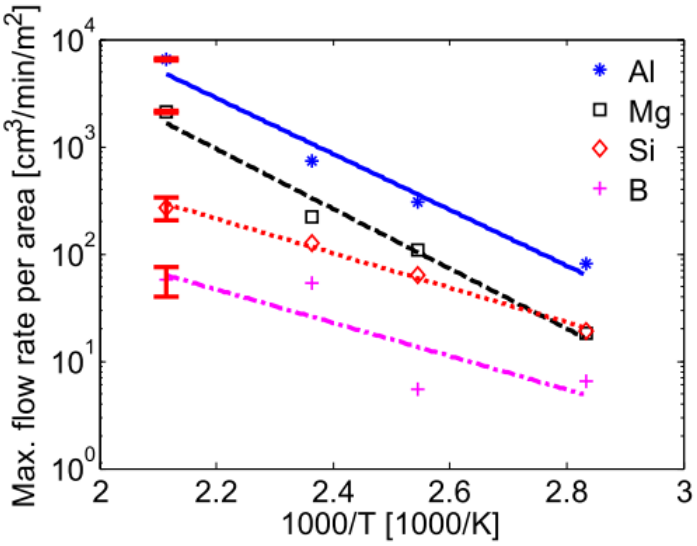

Figure 2.3: Experimental production rate for different metal powders [21].

Each metal exhibits a recognizable pattern in terms of the rate at which hydrogen is produced over time. Initially, there is an induction period during which no hydrogen is generated. Following this, there is a phase of progressively increasing hydrogen output until the maximum rate is attained, after which there is a decline in production until it eventually ceases.

2.2. Aluminum - Water Hydrolysis Reaction

Aluminum is widely regarded as one of the most suitable materials for portable hydrogen sources, primarily due to its high generation efficiency, rapid reaction rate, and non-polluting reaction byproducts. Additionally, using waste aluminum products for hydrogen production can significantly reduce the overall cost. The hydrogen generated by the reaction between aluminum and water has numerous applications in space, as it eliminates the need for hazardous hydrogen transportation and storage. It should be noted that the type

of aluminum-water reaction that occurs is dependent on the reaction temperature.[19]:

$$2Al + 6H_2O = 2Al(OH)_3 + 3H_2 \qquad (20 - 280\ \ ^\circ C) \tag{2.3}$$

$$2Al + 4H_2O = 2AlOOH + 3H_2 \qquad (280 - 480\ \ ^\circ C) \tag{2.4}$$

$$2Al + 3H_2O = Al_2O_3 + 3H_2 \qquad (above\ 480\ \ ^\circ C) \tag{2.5}$$

Under standard conditions and the stoichiometric reaction, 1 gram of aluminum has the potential to produce 1.36 liters of hydrogen gas, with the only byproduct being aluminum hydroxide. The reaction between aluminum and water is not a single-step process, but rather involves several distinct phenomena. The initial stage is primarily due to the diffusion of oxidizing species through the oxide shell of the particles. The second stage, in which hydrogen production increases, is governed by the mixture's chemical kinetics. The final stage, which involves a slowdown of the reaction, is controlled by the thickness of the oxide or hydroxide layer formed by the unreacted metal core [21].
A challenge in using aluminum powder is that it tends to react spontaneously with air, forming a protective layer of alumina that prevents the powder from reacting with water under standard conditions. Consequently, active aluminum must be prepared to enable it to react with water. There are several methods available to improve the reactivity of aluminum, with the underlying principle of either removing the alumina layer or creating defects on the alumina layer on the surface. These methods include ball milling, alloying, gas atomization, and reactions with alkaline solutions.

Different additives can be incorporated to increase the reactivity of aluminum with water and promote a catalytic effect. This effect can be classified into chemical and physical catalysis. Chemical catalysis is based on the formation of a micro-galvanic reaction between the additive element and the aluminum. Physical catalysis, on the other hand, involves incorporating additives on or within the material. During the reaction with water, these additives will detach from the aluminum surface, revealing new active sites and increasing the reaction area. As a result, the aluminum composite will undergo a structural and reaction area change, catalyzing the reaction with water. For instance, the addition of salts such as KCl or $NaCl$ can be used as an example of how to increase the efficiency of the aluminum-water reaction. These salts decrease the particle size of

the active aluminum composite particles during the ball milling process, which in turn increases their specific surface area. During the reaction with water, the salts dissolve and expose the internal aluminum, leading to an increase in active sites for the reaction. On the other hand, the addition of low-melting-point metals like bismuth can create a galvanic reaction that catalyzes the reaction of aluminum with water. Experimental tests have shown that the most effective formulation for increasing both the hydrogen yield and the production rate is aluminum-bismuth-salt. Other low-melting-point metals can also be used in place of bismuth.

2.2.1. Hydrogen generation adding low melting point metals

As previously discussed, incorporating low melting point metals like Sn, In, Bi, Ga, Hg, and Li into aluminum powder can enhance hydrogen production by promoting a galvanic reaction and facilitating the breakdown of the alumina oxide layer, thus improving reactivity. Moreover, these metals and their oxides are non-toxic. The addition of each metal creates a unique microstructure with the aluminum, which yields varying results in the hydrogen production reaction.
As previously mentioned, the hydrolysis of the $Al - Bi$ alloy is based on the formation of micro-galvanic cells between the anode (aluminum) and the cathode (bismuth). While both Bi and Sn can improve the hydrolysis of aluminum, the catalytic effect of bismuth is superior to that of tin. It has been discovered that the addition of other low melting point metals, such as Zn, can also enhance the hydrogen production. Moreover, Ga and Hg, which are liquid at room temperature, can directly corrode the oxide layer on the surface of aluminum powder [19]. Upon examining the reaction rate, it has been observed that magnesium and lithium are capable of significantly increasing the speed of the water reaction under high temperature conditions. Conversely, it has been found that the $Al - Bi$ alloy exhibits the fastest hydrolysis rate at room temperature [20].

Aluminum - Bismuth and Aluminum - Tin powders

A comparison will be made between the use of bismuth and tin in contrast to pure aluminum [10].
The aluminum powder forms a spherical microstructure with grain boundaries on its surface. However, when aluminum is mixed with 20% bismuth, the Bi-rich phases tend to aggregate on the powder surface, forming large spots that cover it. Additionally, there are small Bi-rich regions within the powder on the aluminum grain boundaries. This system is monotectic, which means there is a miscibility gap. On the other hand, powders composed of aluminum and 20% tin form eutectic structures. As there is no miscibility gap, tin is

evenly distributed on the aluminum grain boundaries.
In both cases, the addition of bismuth or tin results in a reduction of the grain size of aluminum, leading to higher activity in the hydrolysis reaction. When examining the hydrogen generation curves of pure Al, $Al-20Bi$, and $Al-20Sn$, it becomes apparent that pure aluminum is incapable of reaching a hydrogen production yield of 100% due to oxidation during the reaction process in water, whereas the addition of bismuth or tin allows for greater hydrogen production yields.

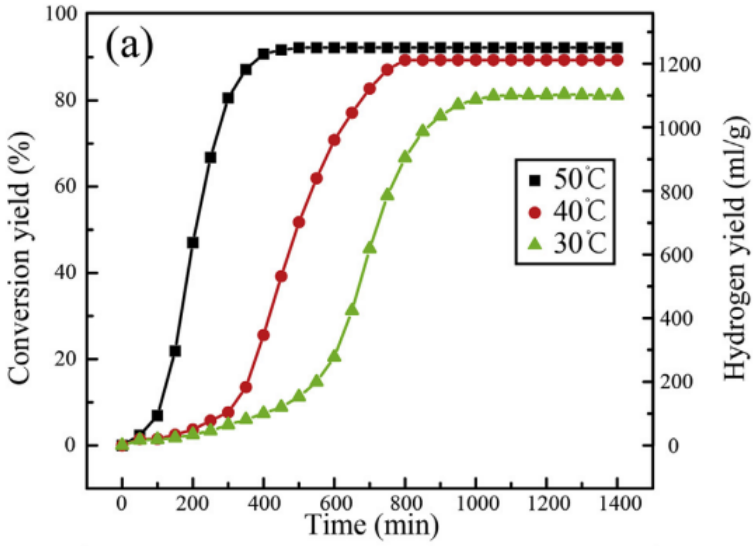

Figure 2.4: Hydrogen generation curve of pure aluminum powder [10].

The $Al-20Bi$ powders exhibit a reaction without any incubation time and can achieve a yield of 100% in the hydrolysis reaction.

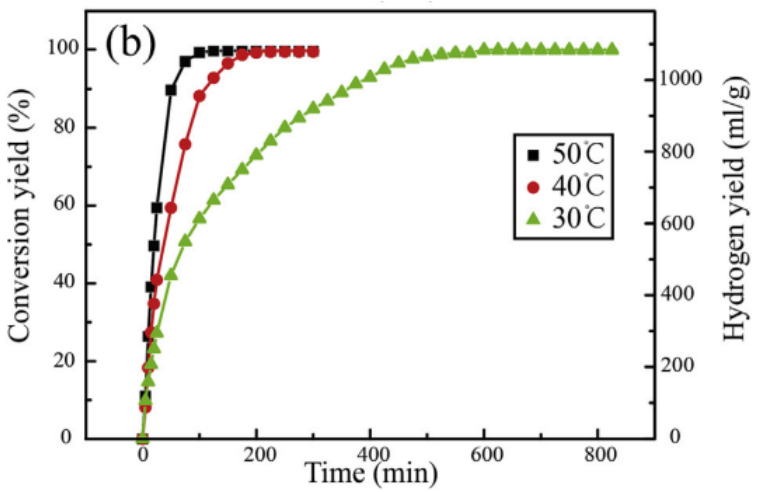

Figure 2.5: Hydrogen generation curve of Al-20Bi wt% [10].

Aluminum powders with the addition of 20 wt% of tin also exhibit enhanced reactivity compared to pure aluminum powders, and can reach a hydrogen yield of nearly 100%.

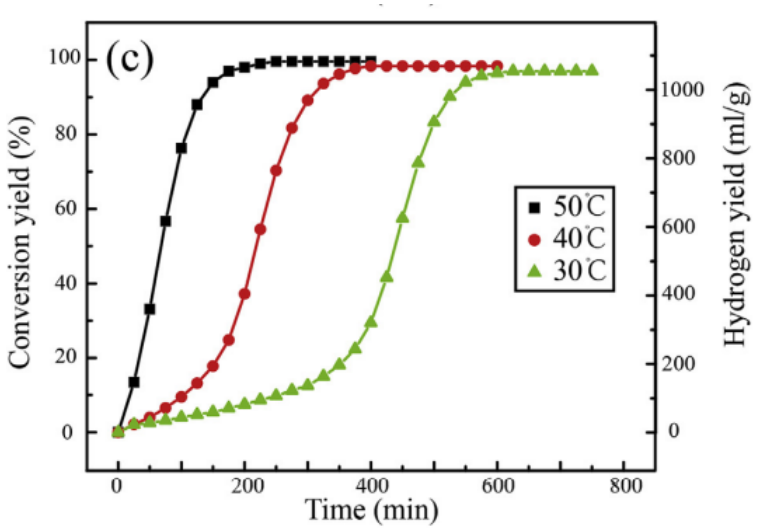

Figure 2.6: Hydrogen generation curve of Al-20Sn wt% [10].

Aluminum activation based on Gallium alloys

Gallam is a gallium-based alloy that can be used to investigate the kinetic properties of activated aluminum reactions by varying the amount and composition of the alloy. Several different compositions of gallam have been tested, including $Ga-In$ (70:30), $Ga-In-Sn$ (62:25:13), and $Ga-In-Sn-Zn$ (50:30:10:10) [7]. By ball-milling with gallam, aluminum was activated and resulted in a fine powder consisting of aluminum particles coated with gallam. This eliminates the oxide film on the surface of the aluminum, allowing it to react with water.

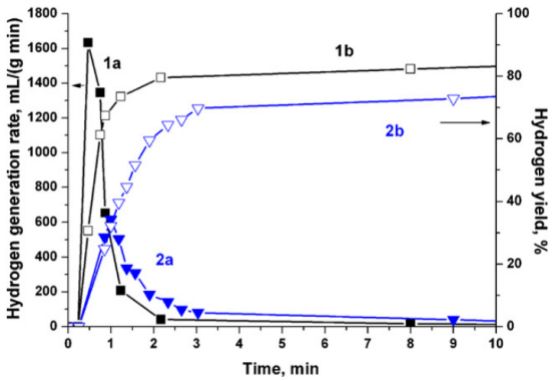

Figure 2.7: Hydrogen yield and hydrogen generation rate for Ga-In gallam (1) manual treatment, (2) high-energy milling [7].

The image depicts the kinetic properties of water-activated aluminum. Curves 1b and 2b illustrate the production of hydrogen, displaying an S-shaped curve typical of a topochemical reaction involving nucleation followed by the growth of a new phase on the surface. The reaction can be segmented into three stages:

1. Induction period: 0,5-4s
2. Fast stage: 0.5-3min
3. Slow stage

In the fast stage, around 70-90% of the theoretical amount of hydrogen is generated, while the rate of hydrogen production is low during the slow stage. Approximately 95% of the total hydrogen yield is produced within the first 1-3 hours. In the third stage, the reduction in the reaction rate is attributed to diffusion limitations, where the reaction products obstruct the penetration of water into the aluminum. The reactivity of aluminum powder is also influenced by the composition of gallam used. All aluminum powders consist of 7% gallam, composed of the compositions previously mentioned.

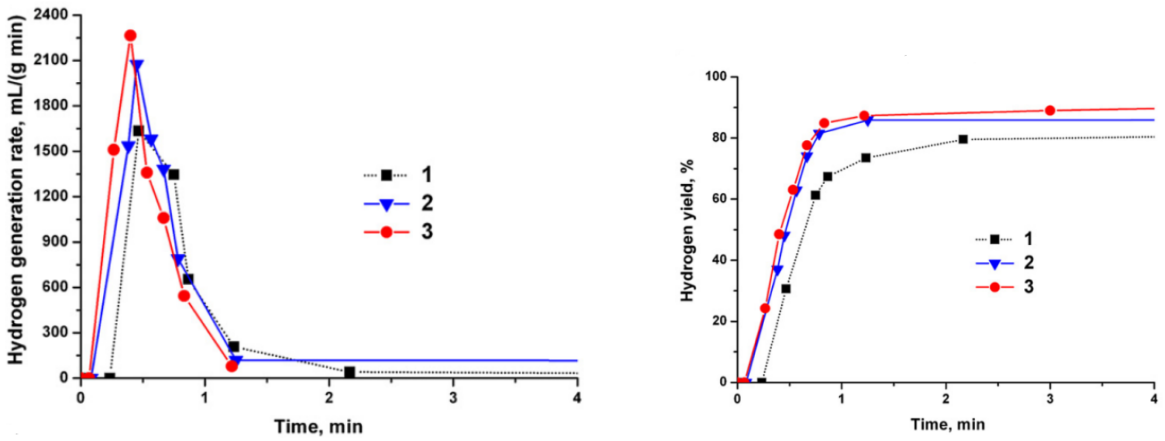

Figure 2.8: Hydrogen reaction kinetics at different gallam compositions (1) Ga-In (2) Ga-In-Sn (3) Ga-In-Sn-Zn [7].

It can be observed that the addition of tin to the $Ga - In$ alloy results in an increase in the reactivity of activated aluminum, while the addition of zinc does not show much difference.

Furthermore, increasing the amount of gallam in the aluminum powder leads to an increase in both hydrogen yield and hydrogen reaction rate, as demonstrated in the following graphs.

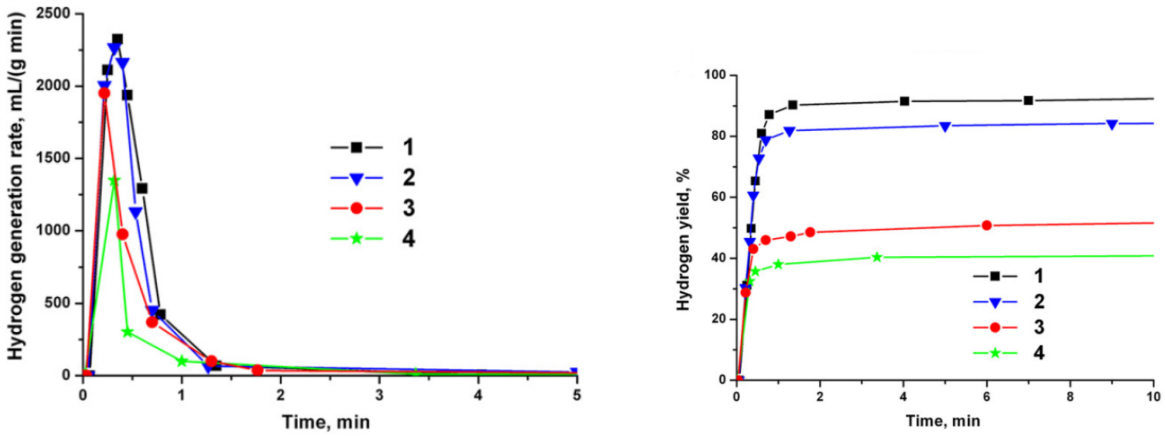

Figure 2.9: Hydrogen reaction kinetics at different gallam's (Ga-In-Sn-Zn) amount wt% (1) 6, (2) 4.3, (3) 3, (4) 2.2 [7].

As anticipated, reducing the amount of the alloy also results in a decrease in both the hydrogen production rate and yield.

2.2.2. Hydrogen generation from Al-Ni mixture

Not only low-melting-point metals, but also metals like Fe, Co, or Ni can react with aluminum to form a galvanic cell, which triggers the aluminum-water reaction. By modifying the $Al - Ni$ ratio in an aluminum powder mixed with nickel, the production of hydrogen can be increased. [22] Powders containing $Al - Ni - NaCl$ can be synthesized using ball milling. The addition of $NaCl$ during mechanical activation can reduce the size of the particles, creating a salt-gate effect that breaks up the aluminum particles, leading to faster reactions with smaller aluminum particles. This enables almost complete consumption of aluminum in water, as $NaCl$ and the Al/Ni micro-galvanic cell promote corrosion.

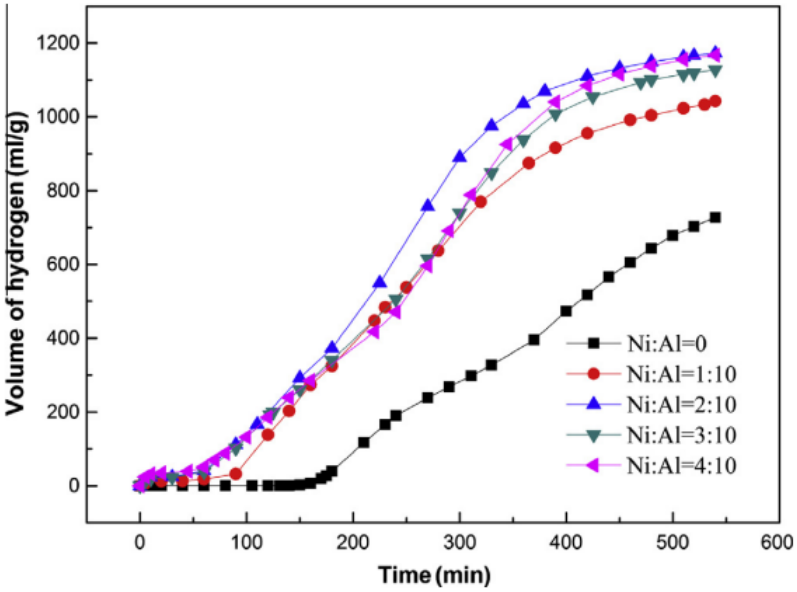

Figure 2.10: Hydrogen generation curves of Al/Ni/NaCl varying Ni ratio [22].

The graph illustrates that the reaction of $Al - NaCl$ without nickel addition is slow, with an induction time of 160 minutes. However, increasing the Ni/Al ratio to 2:10 results in a significant decrease in induction time to 50 minutes. Further increases in the nickel content do not lead to substantial improvements. Additionally, the total amount of hydrogen produced increases from 720 $\frac{ml}{g}$ without Ni to 1170 $\frac{ml}{g}$ with an $Ni - Al$ ratio of 2:10, but a decrease in performance is observed upon further increasing the nickel content. Therefore, the maximum hydrogen yield is obtained with an Ni/Al ratio of 2:10, resulting in a reaction yield of 87.6%, compared to 53.0% without Ni. Despite the weakening of the $Al/Ni/NaCl$ mixture's corrosion in water during the aluminum-water reaction, the addition of nickel can still enhance the corrosion of aluminum.

2.2.3. Al-Fe alloys for hydrogen production

The rate of hydrogen generation from the reaction between aluminum and water increases proportionally with the corrosion or oxidation rate of Al to $Al+$ [4]. The corrosion rate of aluminum can be increased by precipitating an electrochemically noble phase, such as Al_3Fe, along the grain boundaries. This leads to a combined action of galvanic and intergranular corrosion in the Al alloy. Iron is one of the alloy elements that can improve the corrosion rate and is also present as an unwanted material in the range of 1-3% in Al scraps. The surface morphologies of pure Al and $Al - Fe$ alloys, as depicted in the image below, demonstrate that pure Al exhibits a smoothly dissolved surface with shallow

bowls. However, by adding Fe in the range of 1% to 6%, small precipitates form along the grain boundaries, and the precipitate amount significantly increases with increasing Fe content. In particular, $Al-6Fe$ exhibits densely formed, long, needle-like precipitates along and within the grains.

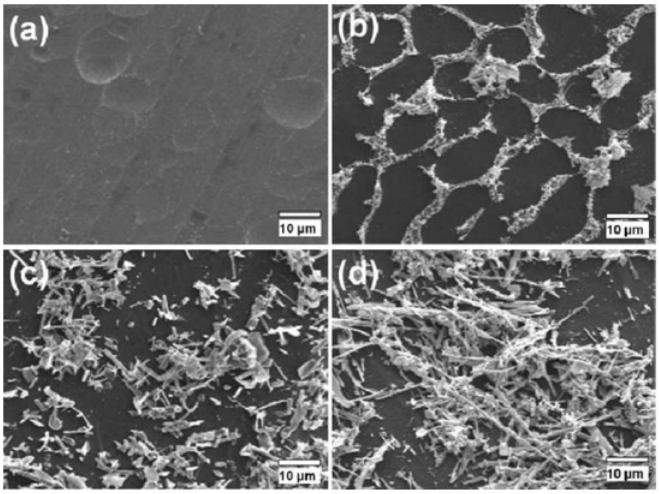

Figure 2.11: SEM images on the surfaces of AL-xFe alloys: a)pure Al b)Al-1Fe c) Al-3Fe d) Al-6Fe [4].

The following image displays both the initial and overall volume of hydrogen generation. The hydrogen generation rate increases significantly by increasing the Fe content from pure Al to $Al-1Fe$. However, upon further increasing the Fe content to $Al-6Fe$, the hydrogen generation rate slightly decreases. The overall results indicate that the rate of $Al-1Fe$ is 3.7 times higher than pure Al, while the rates of $Al-3Fe$ and $Al-6Fe$ are 2.4 times higher than pure Al.

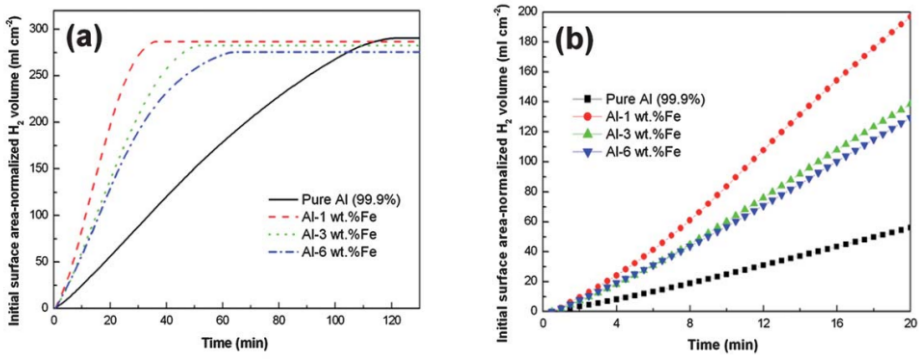

Figure 2.12: Effects of Fe content on the hydrogen generation kinetics of Al-xFe alloys a) overall hydrogen generation reaction b) initial hydrogen generation reaction [4].

The primary reason for the differences in hydrogen generation rates between the alloys is due to their corrosion behavior. Galvanic corrosion occurs when two dissimilar metals with different corrosion potentials are in contact. By increasing the difference in corrosion potential between the two metals, the corrosion rate of the more active metal increases. The active metal, which has a lower corrosion potential, is corroded preferentially, while the noble metal is protected. Since the corrosion potential of Al is much lower than that of other metals such as Fe, Ni, and Sn, when it is connected galvanically to these metals in an alkaline solution, it rapidly corrodes. Therefore, the significant increase in hydrogen generation rates in $Al - Fe$ alloys is due to the galvanic corrosion between the Al phase and Al_3Fe precipitates.

Based on the previous graphs, it is evident that the hydrogen generation rate of $Al-1Fe$ is significantly higher than that of $Al-3Fe$ or $Al-6Fe$, despite having a lower content of Al_3Fe. This could be attributed to the occurrence of intergranular corrosion, which is only possible in the $Al-1Fe$ e alloy. It was estimated that galvanic corrosion and intergranular corrosion account for 65% and 35% of the hydrogen generation rate, respectively.

2.2.4. Ball milling of Aluminum with NaCl particles

To increase the reactivity of aluminum and aluminum alloys, it is necessary to remove the passive oxide layer that forms on their surface and inhibits their reaction with water. One approach to achieve this is by reducing the size of aluminum particles, which increases their surface area and chemical activity. Ball milling is an effective method to break coarse metal particles into a fine powder by causing collisions between balls and particles, which fractures the metal particles [1]. The size of the resulting particles after milling is largely influenced by the mechanical properties of the metal. However, due to the ductile nature of aluminum, milling has a lesser impact on the size of its particles.

$NaCl$ is often used in milling due to its accessibility, affordability, solubility in water, non-toxicity, and eco-friendliness. When the mole ratio of salt to aluminum is increased during milling, the size of aluminum particles can be reduced to the nanoscale, and crystal defects are introduced due to the development of salt gates. This occurs because $NaCl$ is brittle, causing salt particles to fracture during milling and their sharp edges to break aluminum particles into smaller pieces. These factors contribute to an increase in reaction activity, resulting in higher rates and efficiency of hydrogen generation.

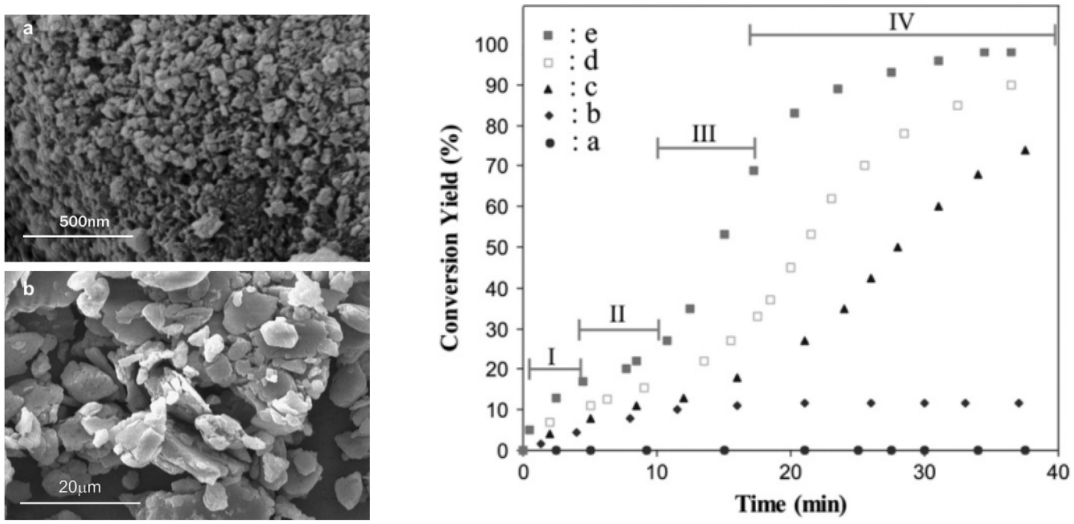

Figure 2.13: Picture 1: SEM micrograph of aluminum powder: a) with salt to aluminum mole ratio of 1.5 b) without salt, Picture 2: Effects of various salts to aluminum mole ratios on the rate and efficiency of hydrogen generation a) 0.1 b) 0.2 c) 0.5 d) 1 e) 1.5 [1].

In Figure 2.13.1, it is demonstrated that the introduction of salt particles to aluminum particles results in a reduction in size of both types of particles. The addition of more salt not only reduces its own size, but also that of the aluminum particles. This process creates additional gates in the aluminum particles, and reducing their size contributes to an increase in the kinetics of the hydrolysis reaction.
Figure 2.13.2 illustrates the impact of varying the salt to aluminum mole ratio. When the quantity of salt is increased, the reaction rate and efficiency also increase. This is due to the brittle nature of salt particles, which fracture during milling. These stiff particles with sharp edges are driven into the aluminum particles, creating local gates that open in a water environment. As a result of the breaking apart of aluminum particles, new surfaces are created, which increase the specific surface area of the aluminum particles. This increase leads to a rise in the rate of hydrogen generation, as the higher surface-to-volume ratio causes more water molecules to be absorbed when the particles are immersed in water.
Figure 2.13.2 shows curves that can be explained as follows: The first region (I) is associated with the rapid generation of hydrogen through the hydration of newly generated surfaces during milling. The reaction is more rapid when the salt to aluminum mole ratio is high because smaller particles have a greater specific surface area. The reaction slows down as an aluminum oxide hydroxide layer forms on the surface. The delay time in region (II) is related to the time needed for the salt gates to be solved, after which

water can reach the aluminum core. A shorter delay time can be achieved by increasing the salt to aluminum mole ratio and obtaining smaller particles. In region (III), after the delay, the rate of hydrogen generation is higher with more gates. In the final region (IV), the aluminum oxide hydroxide layer slows down the reaction rate in newly exposed surfaces. The optimal hydrogen production kinetics are achieved with a salt to aluminum mole ratio of 1.5, which allows the reaction to penetrate the aluminum core particles and increase efficiency up to 100%.

Effects of milling time

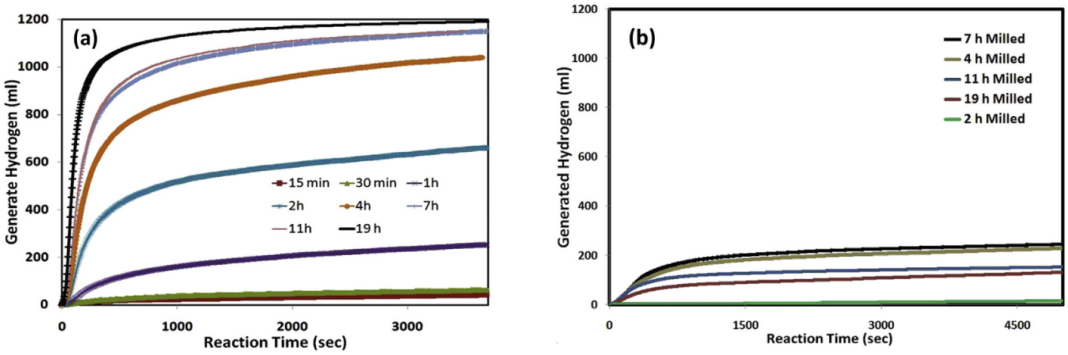

Figure 2.14: Effect of milling time on hydrogen generation of a) the aluminum-salt mixture b)pure aluminum during the reaction with hot water [17].

The impact of milling time on the generation of hydrogen in aluminum-salt mixtures through the reaction with hot water is demonstrated in Figure 2.14(a) [17]. It is evident that hydrogen generation is not observed without ball milling. A short duration of ball milling, such as 15 or 30 minutes, is sufficient to generate measurable hydrogen. An increase in milling time from 1 hour to 7 hours leads to a significant rise in the rate of hydrogen generation. However, further increasing the milling time to 19 hours does not result in a significant increase in the amount of hydrogen generated, since the 7-hour milling time already approaches the theoretical limit. Figure 2.14(b) displays the hydrogen generation outcomes for pure aluminum powder milled for various durations. A comparison of the two graphs highlights the effect of sodium chloride on the hydrogen generation rate. Aluminum milled in the presence of salt reacts much faster than pure aluminum, and the total amount of hydrogen produced is much greater.
It is worth noting that the presence of salt alone, without milling, was ineffective in generating hydrogen. Neither pure aluminum nor salt-aluminum mixtures could produce hydrogen without ball milling. This leads to the conclusion that ball milling alone cannot be sufficiently effective without the presence of a water-soluble salt, and the presence of

salt alone cannot be effective without ball milling.

The impact of the salt type

The following graph illustrates a comparison between $NaCl$ and other inorganic salts such as KCl or $BaCl_2$ [8].

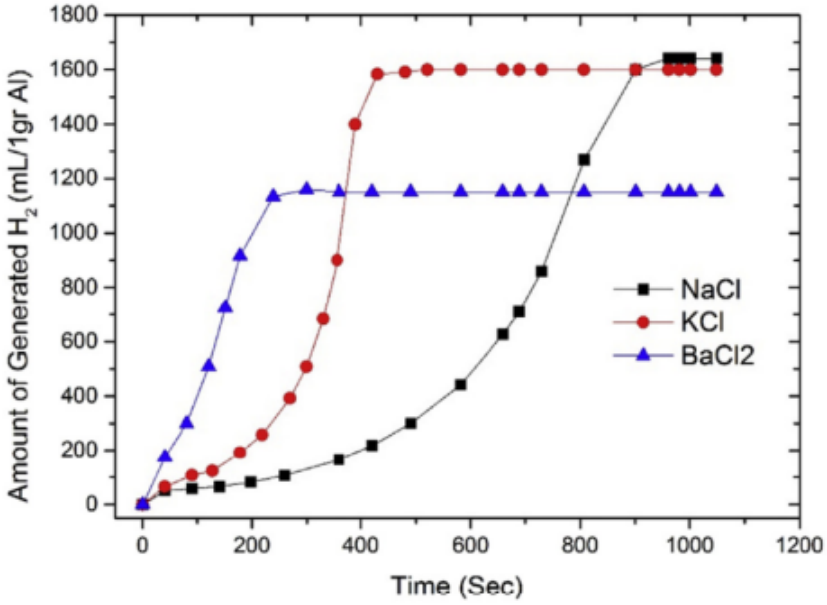

Figure 2.15: Effect of type of salt on the hydrogen generation yield [8].

The presence of $BaCl_2$ was observed to enhance the kinetics of hydrogen production compared to KCl and $NaCl$, as depicted in the graph. As with other aluminum-water reactions, the hydrolysis reaction occurred rapidly in the initial stages, but slowed down as the formation of the passive hydroxide layer impeded the reaction rate. Although samples with KCl had a hydrogen yield similar to those with $NaCl$, the reaction occurred much faster in the former. On the other hand, the sample with $BaCl_2$ yielded the lowest amount of hydrogen, possibly due to its unique microstructural properties and aluminum coating mechanism during ball milling. Overall, the powder containing Al and $NaCl$ exhibited the highest cumulative hydrogen production.

2.2.5. Hydrogen production varying water conditions

Understanding the impact of water on the reaction is an intriguing aspect to explore [2]. Given the abundance of water, it would be practical to examine the usage of alternative water sources in addition to distilled water. In this context, the study compares the hydrogen production yield and reaction rate of three distinct water types: distilled, tap,

and sea water.

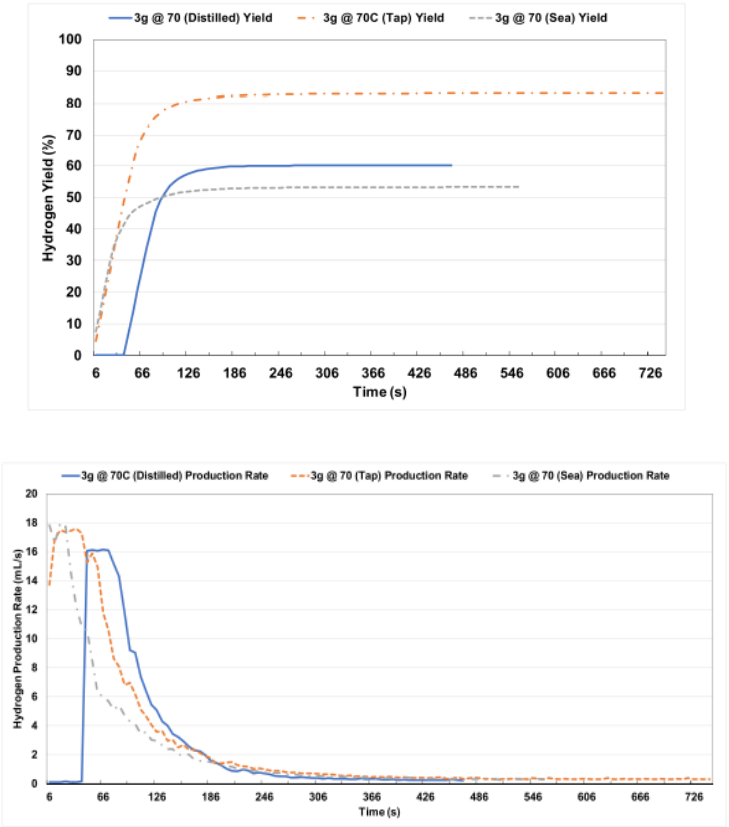

Figure 2.16: Effect of various water mediums on hydrogen generation [2].

The graphs illustrate that tap water achieved the highest yield, exhibiting a reaction efficiency of 83.10% with a 3 g aluminum sample, whereas sea water and distilled water produced yields of only 53.22% and 60.09%, respectively. The superior performance of tap water could be attributed to its mineral and ion composition, which may facilitate the splitting of molecules and the subsequent production of hydrogen.
It is crucial to acknowledge that tap water's composition may differ depending on its location, and hence, the experimental outcomes may vary accordingly. In the present study, tap water exhibited a high concentration of calcium, which could have facilitated the splitting of molecules to generate hydrogen. Conversely, sea water failed to yield significant results due to the presence of several other substances that impede the reaction or do not contribute to hydrogen formation, despite having a higher calcium concentration compared to tap water.

2.2.6. Hydrogen production using an alkaline solution

To prevent the formation of an oxide layer and enable the production of hydrogen via the water-aluminum chemical reaction, hydroxide promoters are employed to create alkaline solutions. This involves the interaction between $NaOH$, aluminum, and water, which can be represented by the following chemical equation [2]:

$$2Al + 2NaOH + 2H_2O \Longrightarrow Na_2Al_2O_4 + 3H_2 \tag{2.6}$$

Sodium hydroxide acts as a catalyst in the hydrolysis reaction of aluminum by promoting the evolution of hydrogen and the formation of bubbles that prevent the precipitation from adhering to the reaction zone. The impact of $NaOH$ as a hydroxide promoter is demonstrated in the following graph [23].

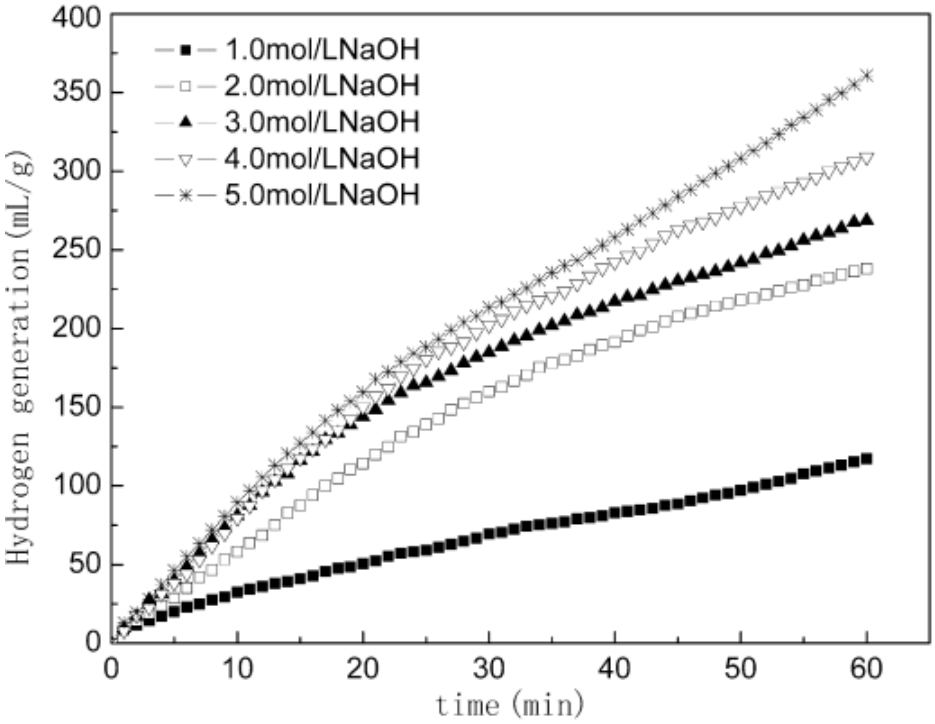

Figure 2.17: Hydrogen generation in different NaOH solutions [23].

Despite the utilization of untreated aluminum resulting in a relatively low total production of hydrogen, the data reveals that augmenting the sodium hydroxide concentration in the alkaline solution leads to an increased yield of hydrogen generation. This is attributed to a greater number of effervescence regions being formed on the aluminum matrix when higher concentrations of $NaOH$ are employed. Additionally, the hydrogen generation rate is higher in solutions with greater concentrations of $NaOH$ due to the quicker dissolution

of the aluminum hydroxide $Al(OH)_3$.
In addition to $NaOH$, KOH can also function as a hydroxide promoter by acting as a catalyst[16]. The following graph presents the results obtained from utilizing various concentrations of $NaOH$ and KOH on aluminum samples with different thicknesses.

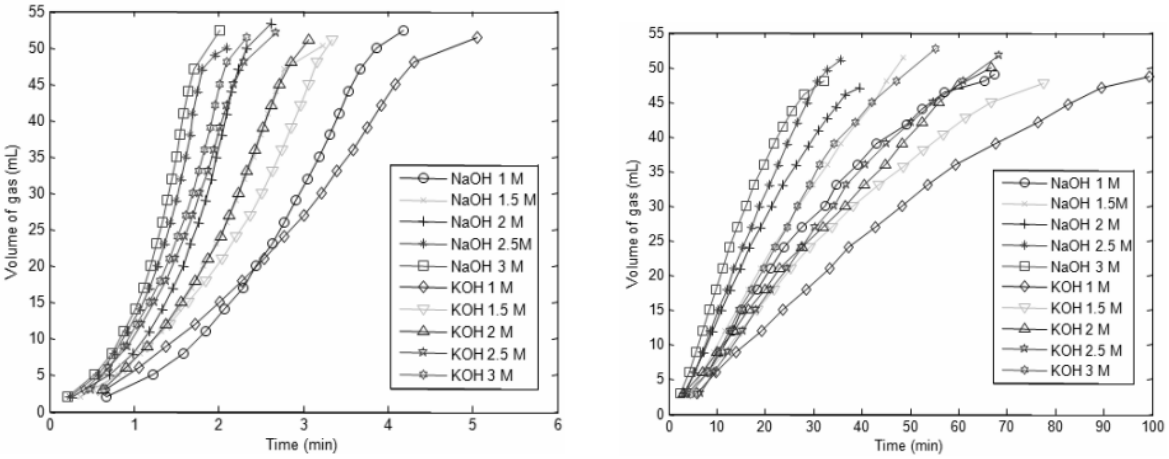

Figure 2.18: Evolution of hydrogen with different catalysts concentration: Picture 1) aluminum foils Picture 2) aluminum plate 0.5 mm thick [16].

An increase in the concentration of the alkaline solution results in a greater amount of hydrogen produced in the same time frame. Furthermore, a comparison of $NaOH$ with KOH reveals that sodium hydroxide has a greater tendency to accelerate the reaction than potassium hydroxide [18]. It can be inferred from the results that the catalytic mechanism varies significantly depending on the type of alkali used. One possible explanation for the observed faster reaction with $NaOH$ compared to KOH is the difference in activation energies. Additionally, all curves exhibit a similar pattern with a rapid and almost linear initial phase followed by an asymptotic plateau.
It has been demonstrated that alkaline solutions can enhance the reaction between aluminum and water, however, they also have a significant drawback. The resulting aqueous solution with added hydroxide promoters is highly corrosive, which limits the choice of materials that can be used as the reaction vessel. This corrosiveness eliminates several metal options.

2.3. Magnesium - Water Hydrolysis Reaction

Magnesium can be utilized similarly to aluminum, in that it can undergo a hydrolysis reaction with water to generate hydrogen. As mentioned earlier, magnesium, along with aluminum, is one of the metals that yields the highest production of hydrogen. The hy-

drolysis reaction between magnesium and water to produce hydrogen follows the following formula:

$$Mg + 2H_2O \longrightarrow Mg(OH)_2 + H_2 \tag{2.7}$$

Magnesium is expected to exhibit greater reactivity than aluminum due to its thinner oxide layer. However, when magnesium reacts with water, the reaction is quickly impeded by the formation of a passive layer of magnesium hydroxide on the reactive material [5]. Generating hydrogen by reacting magnesium with an acid solution can be achieved quickly, but it poses the risk of corroding and damaging the reaction equipment due to the highly corrosive nature of the acid reagents. As a result, activating magnesium powders using acid is not a straightforward process. Ball milling, on the other hand, is a viable method for enhancing the reactivity of magnesium. It disrupts the oxide film and generates a substantial amount of grain boundaries and dislocations. However, ball milling of magnesium results in a significant increase in the particle size of the magnesium alloys compared to raw magnesium powder. This is because, during the milling process, magnesium particles can fuse together through cold welding due to magnesium's high ductility [19]. In the case of magnesium particles, no significant structural modifications occur even when the milling time is substantially increased.

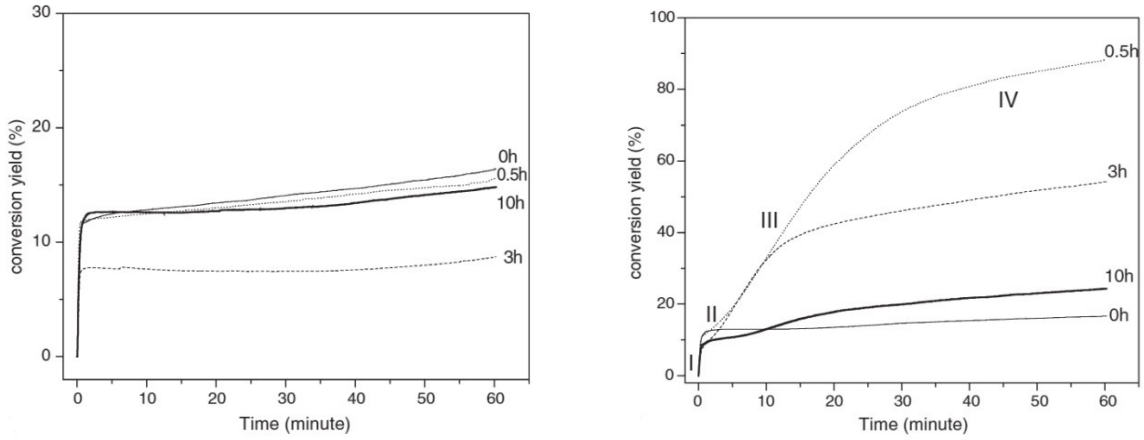

Figure 2.19: Picture 1) Hydrogen production profiles for reaction with pure water [5] Picture 2) Hydrogen production profiles for reactions with 1M KCl [5].

As depicted in Figure 2.19.1, ball milling has no impact on the reactivity of magnesium in pure water. In fact, there is a quick release of hydrogen in the initial 30-60 seconds of the reaction, but then the production rapidly diminishes due to the formation of the oxide layer, resulting in a very low yield of 15%. The outcomes are significantly divergent

if the reaction takes place in a 1M KCl solution. In this instance, the impact of ball milling on magnesium reactivity is substantial. However, the optimal results are achieved with a milling time of 30 minutes, indicating that excessively long ball milling is counterproductive for magnesium powders, leading to a substantial increase in particle sizes. An additional advancement for magnesium hydrolysis reaction can be accomplished by incorporating low-melting point metals. These metals can induce a potent galvanic corrosion rate and generate micro-galvanic cells. In fact, low-melting point metal is utilized as the positive electrode while Mg functions as the negative electrode. The addition of a catalyst can considerably enhance the hydrolysis reaction rate, and moreover, the exothermic reaction can accelerate the hydrolysis rate. The subsequent figure demonstrates the findings of incorporating various low-melting point metals to magnesium powder.

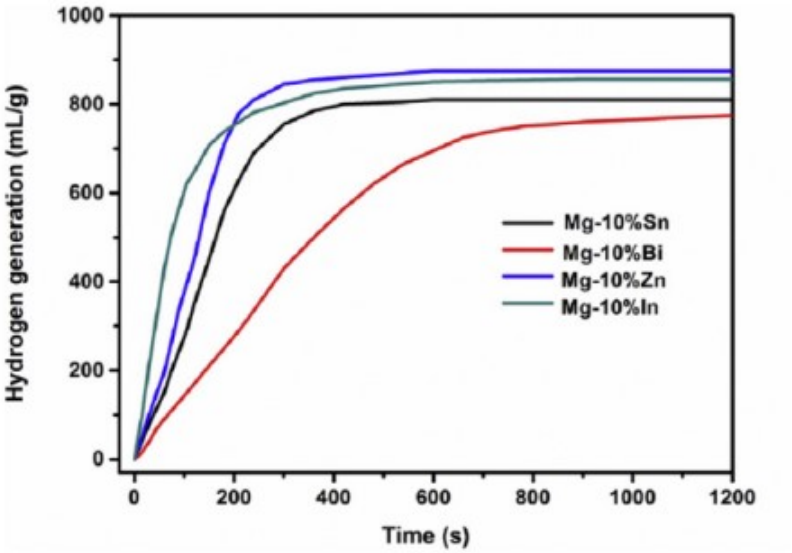

Figure 2.20: Hydrogen generation curves of activated Mg alloys with different low melting point metals [19].

The addition of zinc has been found to yield the best hydrolysis performance, with a reaction yield of 95%. Similarly, the addition of indium as a catalyst also works well, resulting in a reaction efficiency of 93%.

2.4. Effect of varied reaction temperatures on hydrogen production

In general, when examining the production of hydrogen from various metals, it becomes evident from the following graph that raising the reaction temperature leads to a corre-

sponding increase in the amount of hydrogen produced. [21]

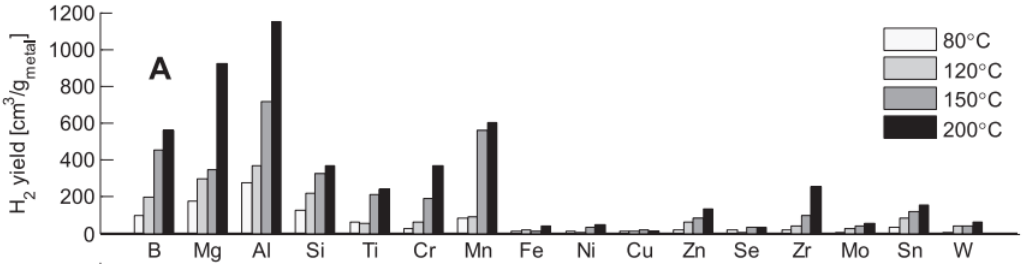

Figure 2.21: Hydrogen yield of experiments conducted at various temperatures [21].

The graph indicates that the highest yield is achieved at 200°C. Furthermore, the powders based on aluminum or magnesium continue to exhibit the most potential, surpassing all other powders by producing over 50%. As temperature increases, the completeness of the reaction also improves, and can even reach 100%. According to the following graph, there are three powders that can achieve complete reaction at a temperature of 200°C.

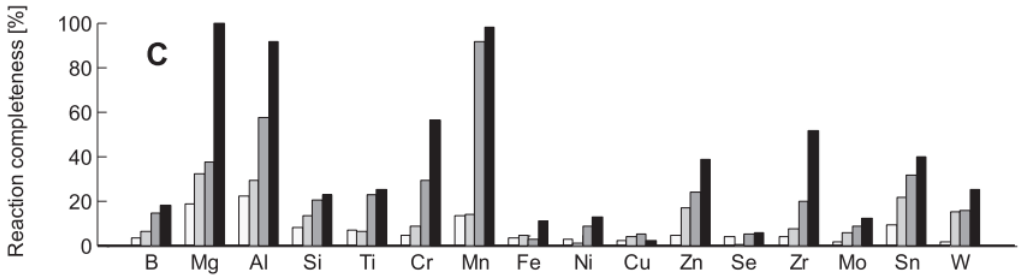

Figure 2.22: Hydrogen reaction completeness at various temperatures [21].

In addition to aluminum and magnesium, manganese is also capable of achieving complete reaction. This is a significant finding because there appears to be a temperature threshold for manganese, where the reaction completeness jumps from 13% to 91% between 120°and 150°Celsius. This phenomenon suggests that certain powders have a temperature threshold above which the reaction completeness is notably improved.

When examining aluminum-based powders with varying additives, it becomes apparent from the following graphs that in each case, the reactivity of the powder dramatically increases with rising reaction temperature.

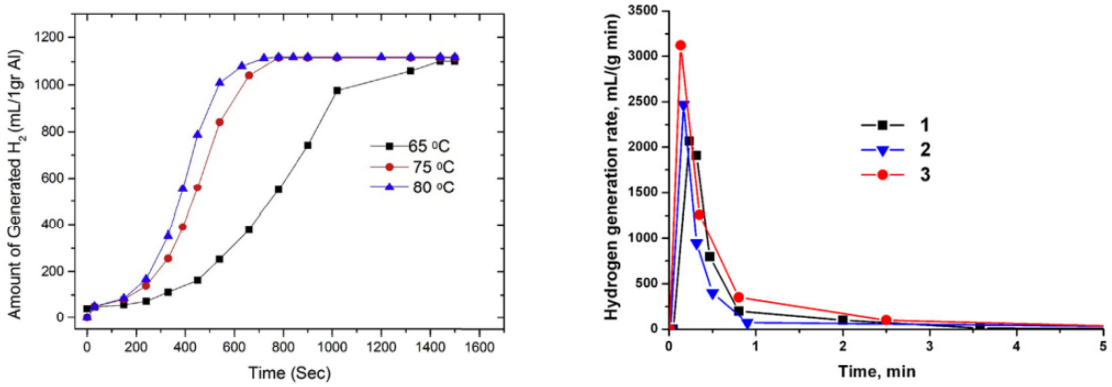

Figure 2.23: Picture 1) Hydrogen generation of Al-2wt%NaCl at different temperatures [8] Picture 2) Rate of the reaction between water and aluminum activated with the Ga-In-Sn-Zn alloy at various temperatures: 1) 21°, 2) 40°, 3)60 °[7].

In Figure 2.23.1, it is demonstrated that the quantity of generated hydrogen increases with rising temperature for a powder comprised of aluminum and 2% $NaCl$. Meanwhile, Figure 2.23.2 illustrates that higher reaction rates are achieved as temperature increases.

3 | Experimental Setup

3.1. Powder and tablet production

3.1.1. Production of the powders

There are three types of powders that have been created, consisting of two varieties utilizing aluminum and the other incorporating both aluminum and magnesium, each with its unique composition:

- **Al** (90%) / **Bi** (5%) / **NaCl**(5%)
- **Al** (90%) / **C**(5%) / **NaCl**(6%)
- **Al**+**Mg**(90%)/**Bi**(5%)/**NaCl**(5%)

The PM100 ball-milling technology was utilized to produce powder blends of varying sizes and morphologies by combining different powders. All blends contained $NaCl$ due to its ability to remove the oxide layer during ball-milling, as well as to reduce the overall powder size due to its brittle nature. All necessary ingredients are combined in a jar alongside the required milling balls, maintaining a ball-to-powder ratio of 20:1.
The air in the jar is replaced with helium as it has been observed that helium aids in eliminating the oxide layer.
The ball milling process lasts for a duration of 6 hours, with a rotation speed of 550 rpm. Each milling cycle lasts for 45 seconds, followed by a 15-second rest period to allow the powder to cool down. This is necessary because mechanical activation leads to an increase in temperature caused by collisions.
The powder containing a mixture of aluminum and magnesium was not subjected to the standard ball milling program of 6 hours because it became overly activated and adhered to the walls of the milling jar, making it unsuitable for water reaction. Therefore, a ball milling program lasting only 2 hours at a speed of 450 rpm was employed instead, using cycles of 30 seconds milling and 30 seconds of rest. Following activation, conservation of the powder in an argon atmosphere is necessary to avoid air reaction and formation of an oxide layer.

3.1.2. Production of the tablets

To manufacture tablets, a pressing machine consisting of two components: the press and the mold, is employed.

Figure 3.1: Hydraulic pump used for pressing the tablets.

Figure 3.2: Pressing structure.

The pressing mechanism comprises a pump, as depicted in Figure 3.1, and the pressing structure. The pump is responsible for pressurizing oil and facilitating its movement through the tube, resulting in the displacement of the piston located at the base of the black cylinder in the pressing structure, as shown in Figure 3.2. The mold is constructed

with two steel blocks fastened by four bolts, and its integral components are the brass and stainless steel pins. These pins serve to compress and shape the tablet inside the mold. The process involves inserting the brass pin into the mold to form the configuration depicted in Figure 3.3. Then, the mold is secured with the bolts, and the powder is poured into the void of the mold. Finally, the stainless steel pin is inserted to complete the process.

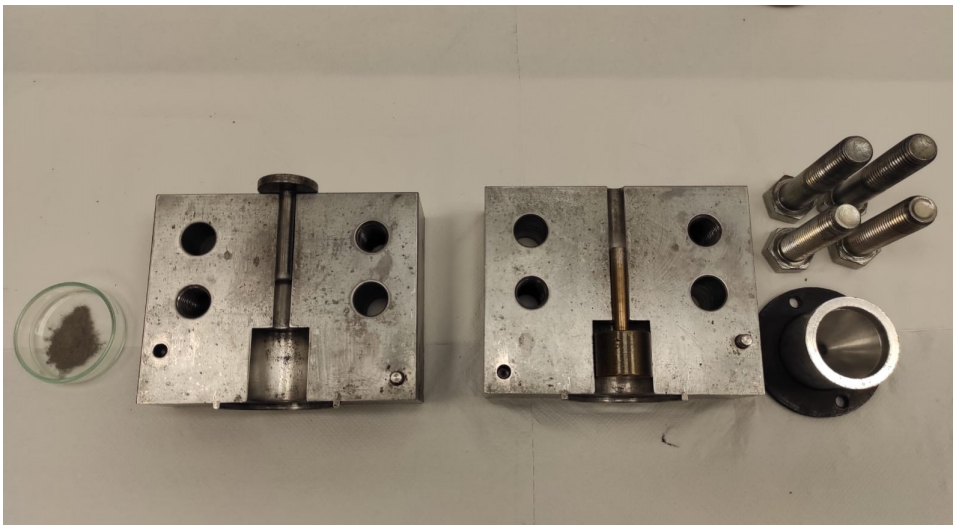

Figure 3.3: The mold.

After the mold is fully closed, it is placed on the pressing machine above the black piston. To secure the mold, the upper portion of the machine made of thick steel plate is fastened onto it. This is achieved by adjusting the nuts, as demonstrated in Figure 3.2, until the upper pin is in contact. The next step involves utilizing the hydraulic pump to activate the piston which pushes the mold upwards. Consequently, the upper pins apply pressure on the powder. Pressing continues for five minutes on one side before rotating the mold to press for another five minutes on the opposite side. This process generates cylindrical, small tablets under a pressure of 100 bar. The resultant tablets, alongside the powder, must be stored in an Argon atmosphere to forestall the formation of a new oxide layer.

3.1.3. Hydrogen Generation Evaluation

According to the aforementioned formulations, the reactants utilized in this reaction comprise of aluminum and magnesium, which yield hydrogen gas when exposed to water. The reaction will be carried out using standard tap water at a temperature not exceeding 280°. Under these specific conditions, the reaction with aluminum takes place in the following manner:

$$Al + 3H_2O \longleftarrow Al(OH)_3 + \frac{3}{2}H_2O \tag{3.1}$$

While magnesium reaction is:

$$Mg + 2H_2O \longleftarrow Mg(OH)_2 + H_2 \tag{3.2}$$

The 3-5nm oxide layer is removed after the milling process to enable the reaction, which requires an assessment of the total hydrogen production, reaction efficiency, and hydrogen production rate. To determine the efficiency of the reaction, it is essential to calculate the theoretical amount of hydrogen attainable from it. This computation involves considering the stoichiometric reaction and recognizing that aluminum, rather than water, is the limiting reactant. The same methodology can be applied to the magnesium reaction by treating it as the limiting reactant and calculating the theoretical amount of producible hydrogen. The theoretical number of moles of hydrogen can be calculated by utilizing the stoichiometric reaction's proportion.

$$1 : \frac{3}{2} = n_{Al} : n_{H_2} \tag{3.3}$$

where:

$$n_{Al} = m_{Al}/M_{Al} \tag{3.4}$$

To determine the amount of hydrogen that can be produced by reacting 1g of aluminum, it will be measured in milliliters.

By using the theoretical hydrogen mole number, one can determine the corresponding theoretical mass of hydrogen through the following equation:

$$m_{H_2} = n_{H_2} M_{H_2} \tag{3.5}$$

In theory, one gram of aluminum has the ability to yield 0.11g of hydrogen.

It is imperative to calculate the theoretical volume of hydrogen that can be obtained from the reaction between aluminum and water, as the total amount of hydrogen generated in the experiment will be measured in terms of volume.

The hydrogen volume is found as:

$$V_{H_2} = \frac{m_{H_2}}{\rho_{H_2}} \tag{3.6}$$

The hydrogen density is found from the equation:

$$P_{H_2} = \rho_{H_2} R_{H_2} T_{reaction} \tag{3.7}$$

where P_{H_2} is the hydrogen pressure and comes from:

$$P_{H_2} = P_{amb} - P_{H_2O} \tag{3.8}$$

P_{H_2O} is the saturated water vapor pressure, and is computed from the Antoine's equation:

$$p_{H_2O} = 10^{A - \frac{B}{C - T_{amb}}} \tag{3.9}$$

The values of constants A, B, and C vary depending on the substance being studied and are determined through experimental methods. For water specifically, the values of these constants are:

A	B	C
8.07131	1730,63	233,426

Table 3.1: Antoine's equation parameters.

When 1 gram of aluminum reacts, it results in the production of 1.22 liters of hydrogen, this is the exact amount of hydrogen that can be generated based on stoichiometry. On the other hand, if magnesium reacts, only 0.0899 g of hydrogen (equivalent to 0.92 liters) can be produced from 1 gram. The actual quantity of hydrogen created can be determined via the water displacement method, which will be discussed in more detail in the following paragraph, with measurements taken in millimeters. Taking all of this data into account, the reaction's efficiency can be calculated:

$$eff = \frac{V_{H_2 real}}{V_{H_2 stoich}} \tag{3.10}$$

Additionally, as the tablet's mass may slightly fluctuate throughout the various experiments, to ensure fair comparison of results, the overall amount of hydrogen produced will be measured in units of grams per kilogram $\frac{g}{kg}$. This method will determine the quantity

of hydrogen produced for each kilogram of aluminum.

To determine the actual quantity of hydrogen generated, use the following equation:

$$m_{H_2} = n_{H_2} R_{H_2} \tag{3.11}$$

where:

$$n_{H_2} = \frac{P_{H_2} V_{H_2}}{R_u T_a m b} \tag{3.12}$$

In addition to the overall quantity and efficiency of hydrogen production, it will also be calculated the rate of the hydrogen reaction.

In order to determine the overall efficiency of the reaction when magnesium and aluminum are combined in a single powder, it is necessary to treat each element separately based on its respective reaction formula.

3.1.4. Experimental Setup and Procedure

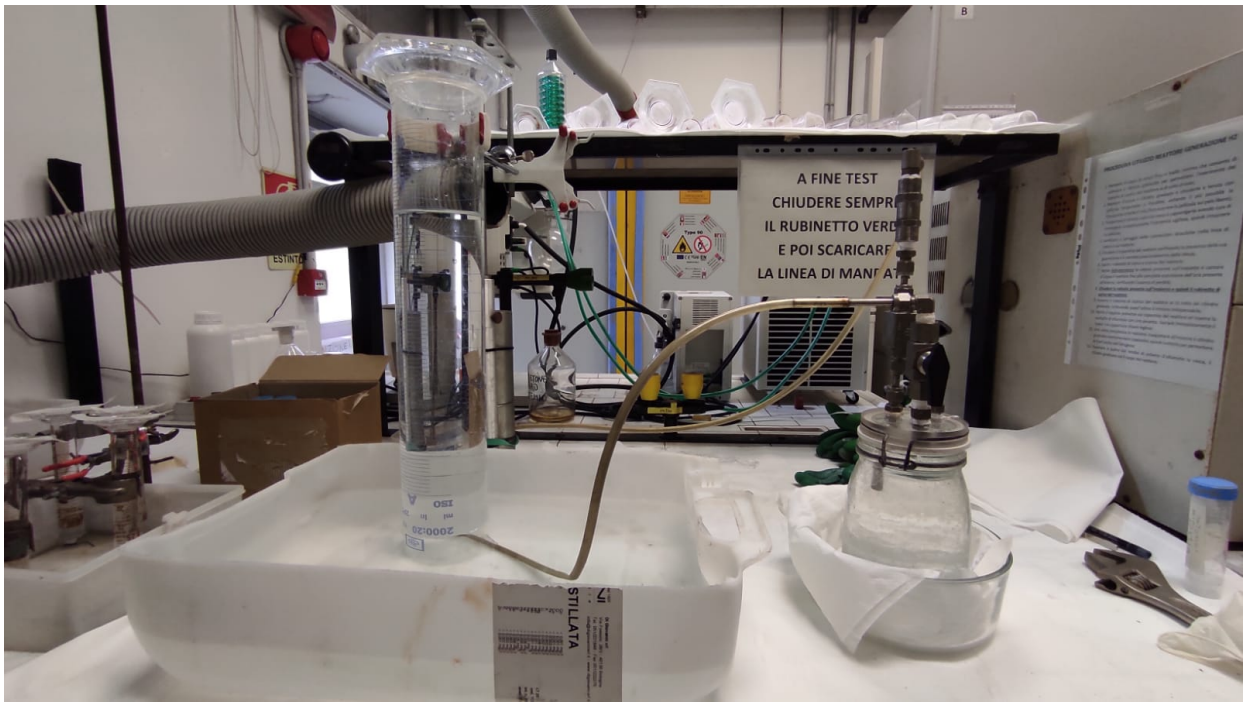

Figure 3.4: Experimental Setup.

The experimental arrangement is identical to what Marotto utilized[13].
The hydrogen production process consists of two parts, namely the reactor and the reading column, and the amount of hydrogen generated is determined by utilizing the water

displacement method.

The tablet reaction with water to create hydrogen occurs within a jar known as the reactor. This jar receives its water supply from the laboratory's main source and is initially filled to capacity with tap water at room temperature. Any remaining air in the container and the connecting tube between the reactor and the reading column is purged by the continued flow of tap water until it is fully eliminated. Following this step, both the general water supply and the tap are closed, and the connecting tube is positioned beneath the reading column, as demonstrated in Figure 3.4.

The column used for reading graduation in the $Al-Bi-NaCl$ powder has a capacity of 2 l, while the other two powders require a 250 ml column due to their low reactivity, which provides more accurate measurement of water displacement. The column is filled to the brim with water and turned upside down in a container of water to seal it. To maintain accuracy of experimental results, it is critical to fill the column with caution and prevent the formation of air bubbles.

The reaction can begin once the reactor and reading column are both filled with water and connected together. To start, a tablet enclosed in a paper package and secured with copper wire is placed in the reactor. It's important to weigh the tablet before commencing the reaction. Hydrogen produced during the reaction is collected in the reading column and its rate and overall amount are evaluated periodically. Temperature and pressure measurements are taken before and after the experiment. To obtain accurate results, the hydrogen trapped at the top of the reactor and inside the tube needs to be accounted for by opening the water supply tap and pushing the trapped hydrogen into the reading column, as was done with the trapped air at the start.

Tablet insertion in water

Once the reactor is completely filled with water and any trapped air has been removed, a tablet must be inserted. There are two methods to accomplish this task. The first involves placing the tablet directly into the water through an opening on the upper part of the reactor. The second method entails placing the tablet in a paper package, which is then sealed with a copper wire and inserted into the reactor.

The primary difference between these two methods is that in the first, the tablet dissolves quickly after the reaction begins and disperses throughout the approximately 1 liter of water in the reactor. Additionally, some of the reactable aluminum may pass through the connection tube and reach the reading column, resulting in a loss of aluminum. In contrast, the second method involves the tablet breaking apart immediately after the reaction starts, but remaining confined within the paper package. Consequently, different results can be obtained using this method.

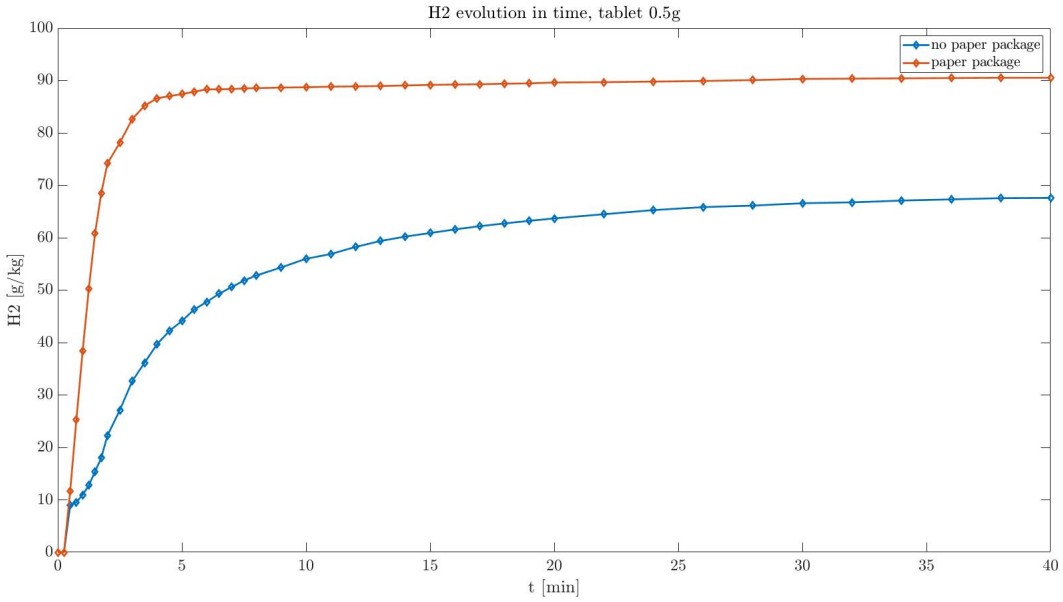

Figure 3.5: Hydrogen evolution in time.

There are significant discrepancies between the two methods of tablet insertion in water. It is worth noting that placing the tablet in the paper packaging results in a higher hydrogen yield of approximately 90%, while leaving the tablet unenclosed in the water leads to much lower efficiency of around 60%. This experiment was conducted on the $Al - Bi - NaCl$ mixture, but the same pattern was observed with other formulas. The considerable variation in total hydrogen production can possibly be attributed to the fact that using the paper package ensures all the powder stays in one place, whereas placing

the tablet directly in the water results in some powder being carried away by the hydrogen as it moves from the reactor to the reading column, thus some of the reactive powder is lost in this way.

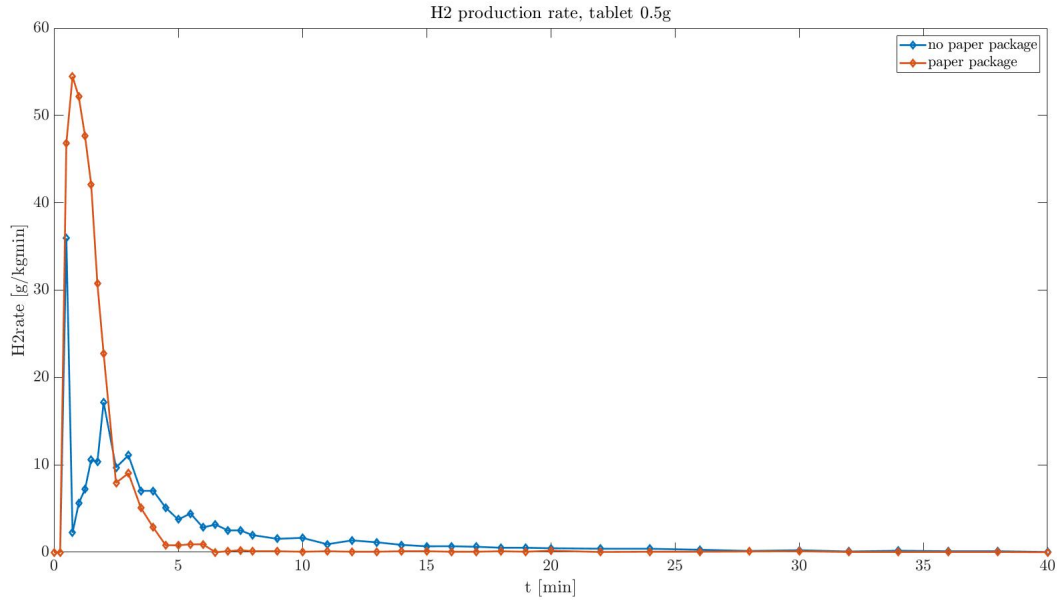

Figure 3.6: Hydrogen production rate.

Using a paper package can significantly accelerate the hydrogen production rate. This could be due to the concentration of the powder in one area, leading to localized temperature increases and a corresponding increase in production rate. Directly mixing the tablet with the water, on the other hand, results in a much larger amount of water involved in the reaction, which can hinder the rate of reaction compared to the stoichiometric value. Furthermore, the reaction rate of the powder without the paper package is different from that with the paper package, showing two distinct production peaks in comparison to the immediate peak and subsequent slowdown seen with packaging.

3.2. Al-Bi-NaCl powder

The initial powder tested consists of 90% Al, 5% Bi, and 5% $NaCl$, with the inclusion of Bi acknowledged in the literature for enhancing the reaction of aluminum with water to produce a galvanic cell, and $NaCl$ added for ball milling in order to decrease the size of aluminum particles. The final outcome presented in the following table is obtained from the median of three experiments on three distinct tablets, each made with a pressure of 100 bar on both sides for an equivalent time, with a total compression duration of 10 minutes and a tablet weight of 0.5 g.

Mass [g]	0.5097
Total H2 produced [g/kg]	96.07
Reaction efficiency %	98.75
Induction time [s]	0
$Time_{90\%}$ [min]	6.5

Table 3.2: Al-Bi-NaCl tablet result.

$Time_{90}\%$ corresponds to the duration required to achieve 90% of the total hydrogen produced, whereas induction time refers to the amount of time needed for the reaction to commence after inserting the tablet into the water. The hydrogen production trend is illustrated in the following graph:

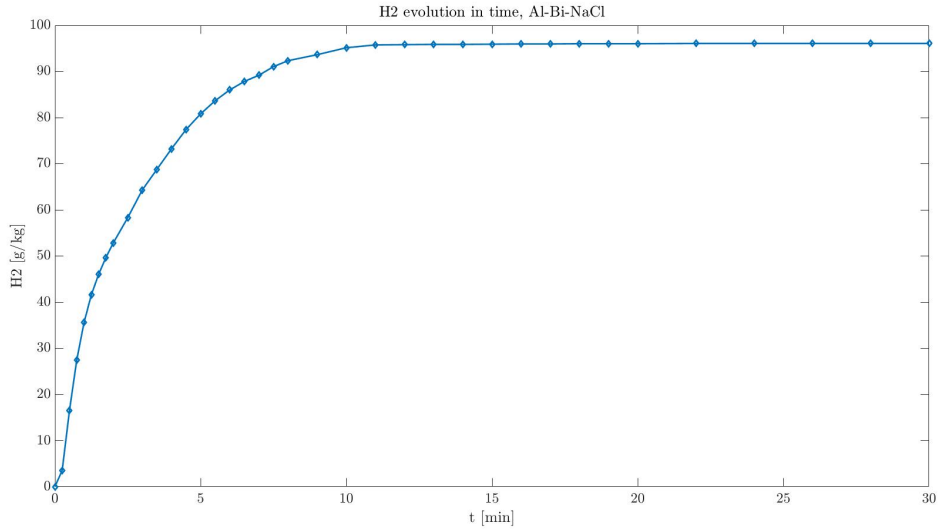

Figure 3.7: Hydrogen production evolution of Al-Bi-NaCl powder.

The results indicate that the induction time is zero seconds, implying that the reaction

starts immediately upon contact of the tablet with water, owing to its high potency. On the other hand, it takes 6 minutes and 30 seconds to generate approximately 90% of the total hydrogen produced. The test lasted for 30 minutes, and no increase in hydrogen production was observed beyond this time. The amount of hydrogen produced was measured in grams per kilogram of aluminum used. Additionally, the reaction exhibited high efficiency, as it achieved an overall yield of almost 100%, which suggests that almost the stoichiometric amount of hydrogen was produced.
The evolution of hydrogen over time bears a striking resemblance to how aluminum powder behaves in water. Initially, the reaction is swift and transient, after which the tablet behaves like powder, uncompressed, leading to a sudden surge in hydrogen production. This behavior stems from the reaction's intensity, which causes the tablet to break apart rapidly, returning to its original powder state. The ensuing hydrogen production rate trend is illustrated below.

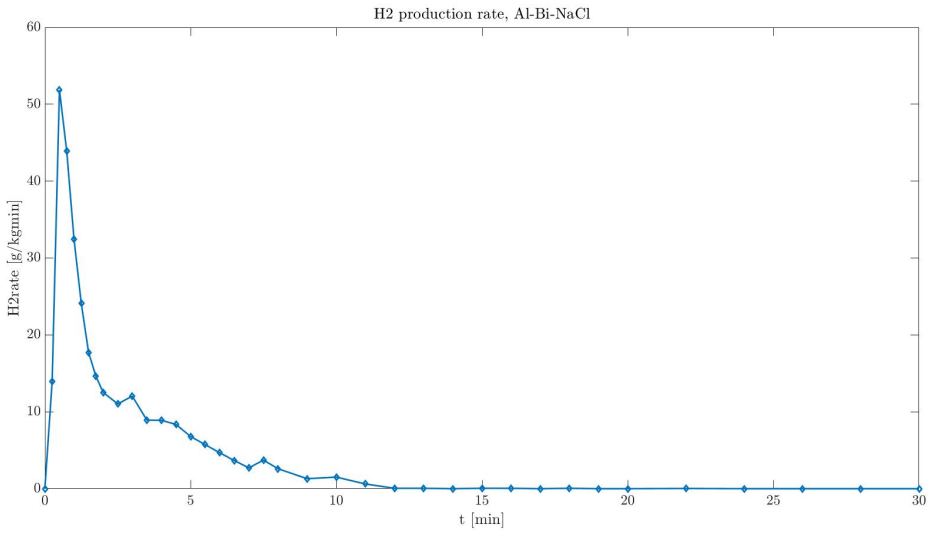

Figure 3.8: Hydrogen production rate of Al-Bi-NaCl powder.

The initial stages of the reaction show a high speed, generating nearly all potential hydrogen within a mere 6.5 minutes. This is evident in the peak observed in the initial production rate. As a significant proportion of the reaction is executed, the rate gradually approaches zero.

3.3. Al-C-NaCl powder

The powder made of a combination of Al, C, and $NaCl$ is distinct from the initial powder tested solely due to the replacement of bismuth with graphite. The overall composition, which contains a matching percentage of aluminum and salt, has been employed to enable the comparison of various results achieved and determine the optimal powder. According to literature, the inclusion of graphite in aluminum powder should heighten its interaction with water, resulting in the production of hydrogen. [6] Milling is still done using $NaCl$ as the agent. The mixture consists of 90% aluminum powder, 5% graphite, and the remaining 5% salt. By incorporating graphite, an e-shell structure is formed around the aluminum particles, facilitating the hydrogen generation reaction at the interfaces. To investigate the reaction trend, three experiments were conducted using 0.5 g tablets, which were pressed for 10 minutes at 100 bar pressure on both sides. However, caution must be exercised when handling tablets made from this powder as they tend to be more brittle. Additionally, it is challenging to obtain tablets with consistent weights since the compression may not result in all the powder being used, leaving some as free powder. In fact, this can be seen with the lower mass of the resulting tablets even though 0.5 grams of powder were used for compression. The test results for this powder are as follows:

Mass [g]	0.4479
Total H2 produced [g/kg]	8.28
Reaction efficiency %	8.47
Induction time [s]	120
$\boldsymbol{Time_{90\%}}$ **[min]**	70

Table 3.3: Al-C-NaCl tablet result.

After testing for 1.5 hours, the hydrogen trend remained constant and there was no noticeable increase in hydrogen generation. The reaction was highly inefficient, with less than 10% efficiency, indicating that something is inhibiting it. When the tablet was placed in water, it took approximately 120 seconds for the reaction to begin, and it was slow to reach 90% of overall hydrogen production, taking 70 minutes. The evolution of hydrogen production trend is outlined below.

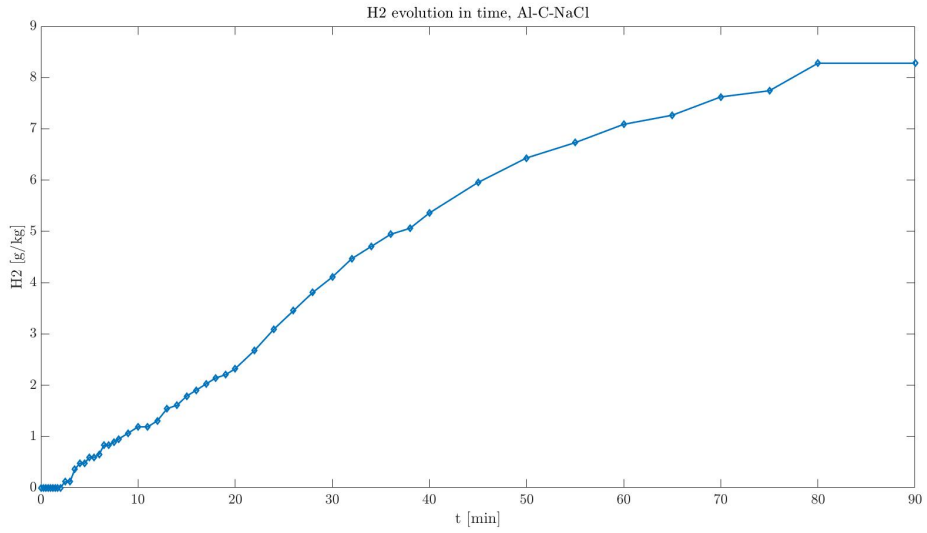

Figure 3.9: Hydrogen production evolution of Al-C-NaCl powder.

The behavior of hydrogen evolution in this scenario does not resemble that of a powder. Instead, hydrogen production exhibits a quasi-linear trend, steadily generating small amounts of hydrogen over an extended period of time. Below is a graph depicting the hydrogen production rate.

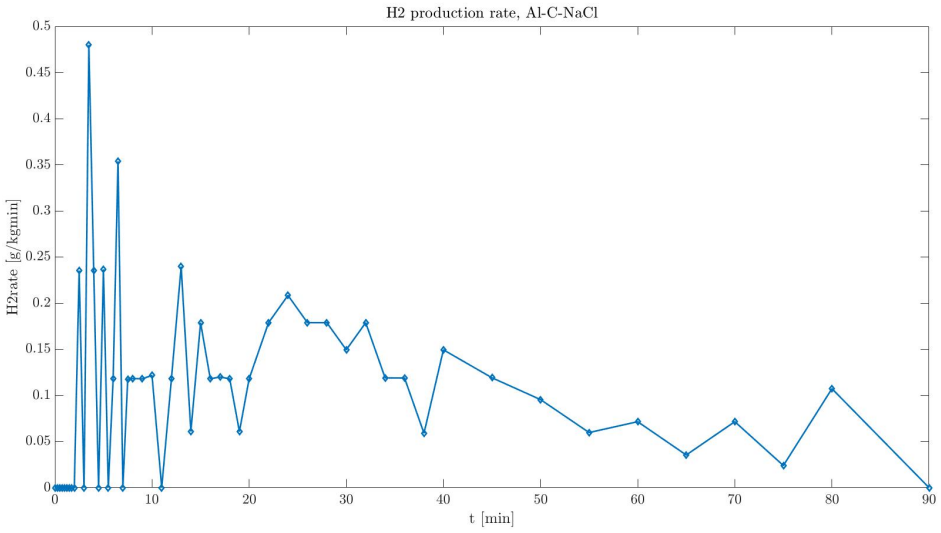

Figure 3.10: Hydrogen production rate of Al-C-NaCl powder.

The graph indicates that the trend is significantly distinct from the one obtained using the $Al - Bi_NaCl$ powder. There is no initial surge in production; rather, the reaction remains consistent after a 2-minute induction period. Moreover, the hydrogen production lacks a consistent pattern, exhibiting peaks and valleys at irregular intervals.

The $Al - C - NaCl$ powder did not yield the expected results, resulting in minimal hydrogen production. The cause could be attributed to two factors: either the proportion of graphite used was too low to initiate the reaction, or the powder was not activated enough, indicating the need for an extended milling time. The trials were not conducted at room temperature, but rather with water cooled to varying degrees between 45°and 50°, since this composition does not respond at water temperatures less than 35°. Furthermore, due to the reaction's feeble nature, the tablet did not break, remaining intact throughout the entire process. This likely restricted the opportunity for the tablet's internal regions to react.

3.4. Mg-Al-Bi-NaCl powder

The powder containing Mg, Al, Bi, and $NaCl$ replicates the composition of the prior powders. Specifically, 90% of it is a combination of Mg and Al, with the remaining 10% being divided equally between Bi and salt. Within the 90% Mg and Al mix, Mg accounts for 60% and Al accounts for 40%. Bismuth remains present to facilitate the formation of a galvanic cell with magnesium and aluminum and to enhance their reaction. Salt is included again as a milling agent, as this composition is also activated by ball milling. However, the ball milling program for this powder was modified compared to the other two, as the powder became too activated and the particle size increased due to magnesium cold welding following an overall milling of 6 hours. Instead, a 2-hour ball milling was employed, resulting in a similar powder as the other two compositions. These tablets were also compressed at a pressure of 100 bar and exhibited a brittle composition similar to those made from the $Al - C - NaCl$ powder. Consequently, additional powders were required to produce 0.5 g tablets, as some particles could not be compressed and remained free. Three experiments were carried out, and their median results are listed below.

Mass [g]	0.501
Total H2 produced [g/kg]	11.95
Reaction efficiency %	14.43
Induction time [s]	60
$\boldsymbol{Time_{90\%}}$ **[min]**	210

Table 3.4: Mg-Al-Bi-NaCl tablet result.

The reaction was monitored for 5 hours due to the sluggish yet steady hydrogen production. After 4.5 hours, a halt in hydrogen production was observed, with 90% of total hydrogen being generated in the initial 3.5 hours. Additionally, a 1 minute induction

time was required before the production of the first trace of hydrogen. In any case, the reaction efficiency is relatively low, yielding only 14.43% of the theoretical amount of hydrogen. This suggests that an inhibiting factor is at play, as the combined magnesium and aluminum powder was never tested. One potential cause of inhibition may be an excessively high level of powder activation, despite reducing the milling time from 6 to 2 hours. Alternatively, water may be impeding the magnesium reaction by facilitating the formation of an oxide layer. The forthcoming graph will display the hydrogen production over time.

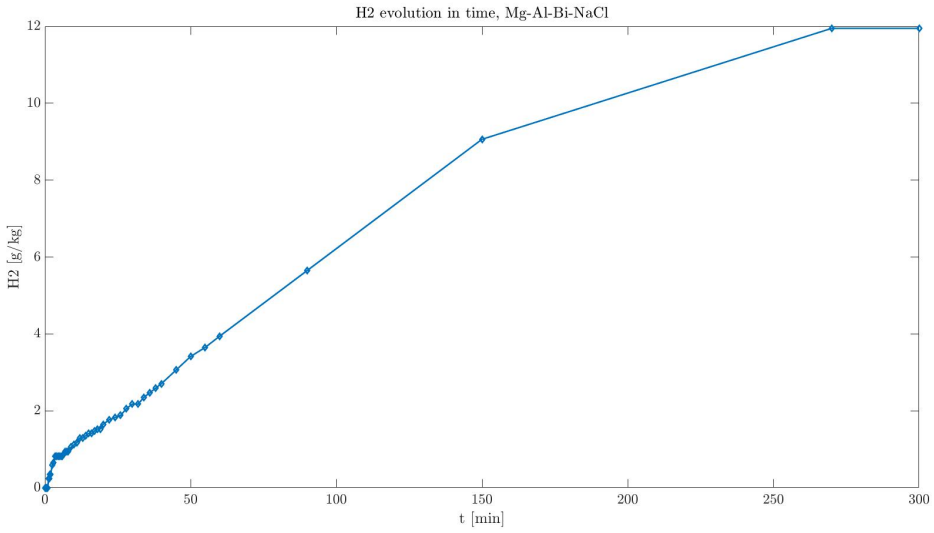

Figure 3.11: Hydrogen production evolution of Mg-Al-Bi-NaCl powder.

The hydrogen production process in this case is similar to that of the $Al - C - NaCl$ powder, demonstrating a quasi-linear trend due to the gradual release of hydrogen over time. However, the reaction is not strong enough to break the tablet, resulting in limited reaction occurring only on the outer surface. This may explain why the quantity of hydrogen produced is low. The graph below indicates the hydrogen production rate, which is distinct from previous powders. Unlike the instantaneous peak observed with other powders, this powder displays multiple peaks after an induction period, indicating an inconsistent reaction rate. The reaction slows down after 60 minutes and ultimately reaches a zero production rate after 5 hours.

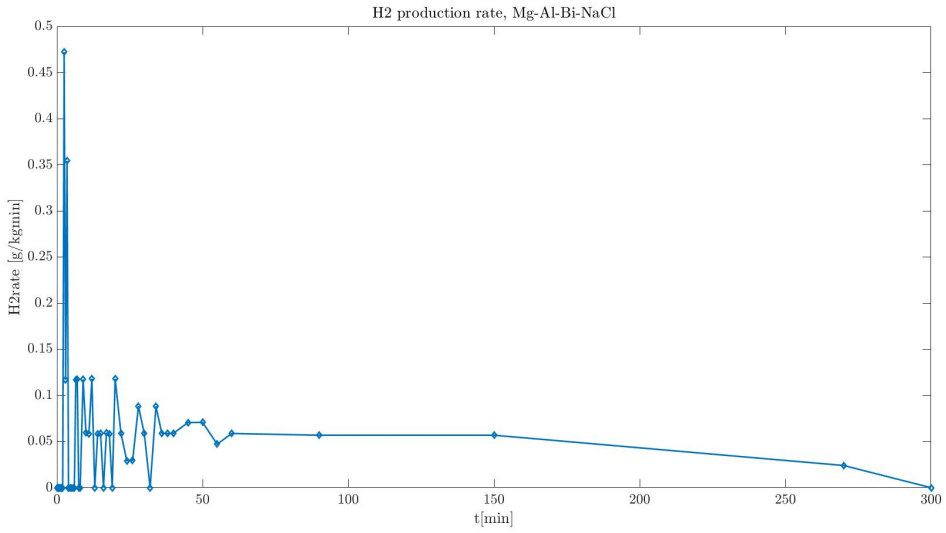

Figure 3.12: Hydrogen production rate of Mg-Al-Bi-NaCl powder.

3.5. Hydrogen production comparison

After conducting tests on three different powders, it was found that they yielded significantly diverse results. The powder comprising of $Al - Bi - NaCl$ exhibited the most favorable outcome, and had a production pattern distinct from the other two powders. Conversely, the powders comprised of $Al - C - NaCl$ and $Mg - Al - Bi - NaCl$ displayed a strikingly similar trend. These results are depicted in the following graph.

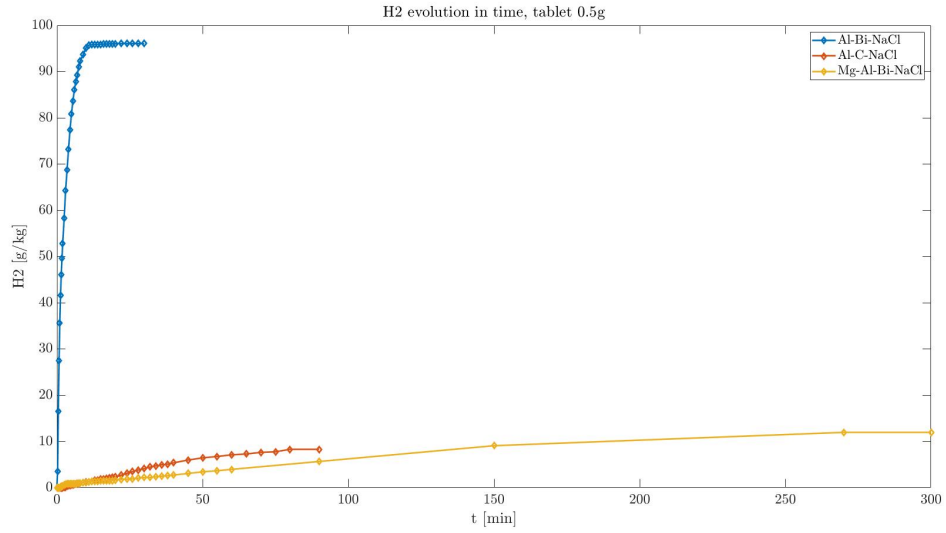

Figure 3.13: Hydrogen evolution comparison between Al-Bi-NaCl, Al-C-NaCl and Mg-Al-Bi-NaCl powders.

It is worth noting that each of the three powders underwent different lengths of testing due to their individual kinetics. The $Al-Bi-NaCl$ powder yielded the highest efficiency and quickest hydrogen production, with almost 100% of the theoretical amount generated in just 30 minutes of testing. The reaction was so swift that once the tablet came into contact with water, the reaction occurred rapidly, resulting in the tablet transforming into powder. Furthermore, the reaction was so efficient that there was no further hydrogen production beyond the initial reaction. The other two powder types underwent a longer testing period. One of them, consisting of $Al - C - NaCl$, was tested for 90 minutes until it appeared that the reaction was complete. Although the reaction in this instance progressed slowly, there was insufficient power to completely break down the tablet into powder form. Consequently, only the external portion of the tablet reacted with water, leading to a comparatively low reaction efficiency. Furthermore, there appears to be an inhibiting factor present in this formulation. Similarly, the powder comprising of $Mg - Al - Bi - NaCl$ undergoes a similar reaction with the only distinction being that it manifests over a longer duration, having been tested for five hours due to a gradual and consistent hydrogen production. After the five-hour mark, there was no observable increase in the volume of hydrogen produced, and the tablet remained intact throughout the reaction. The combined composition of Mg and Al has never been examined, so there may be hindrances that impede the reaction from finishing. Powder activation through ball milling may also be problematic, leading to an overly activated powder. A table comparing the reaction efficiencies of the three powders is included below.

	Reaction efficiency [%]
Al-Bi-NaCl	98.75
Al-C-NaCl	8.47
Mg-Al-Bi-NaCl	14.43

Table 3.5: Powders reaction efficiency comparison.

3.6. Powders Characterization

3.6.1. XRD Analysis

Figure 3.14 shows the XRD analysis of powder and tablet composed by $Al - Bi - NaCl$. In the powder sample it is possible to identify the characteristics diffraction peaks of Al,Bi and $NaCl$. In particular the peaks at a 2θ of 77.89°, 65.02°, 44.70° and 38.26° correspond to an intensity of 311, 220, 200 and 111 for aluminum. Considering bismuth, it shows peaks at 2θ values of 70.73°, 62.43°, 56.00°, 48.53°, 39.61° and 26.95° for an intensity of 214, 116, 024, 202, 104 and 012. Instead, $NaCl$ has a peak at a 2θ of 31.70° with an intensity of 200. The powder composition does not exhibit any diffraction peaks related to metal oxides or hydroxides. This suggests that the ball-milling treatment does not have any impact on the composite's phase composition.

Considering the diffractogram of the tablet, it is noticed also the presence of Al_2O_3 which is corundum and Bi_2O_3 or $Bi(OH)_3$. In particular, Al_2O_3 shows two peaks at a 2θ of 42.56° and 36.05° with an intensity of 113 and 110. Bi_2O_3 shows diffraction peaks at a 2θ of 28.58°, 30.07° and 32.01° with an intensity of 201, 220 and 220. Based on these findings, it can be observed that the use of pressure during tablet production is responsible for the creation of metal oxides.

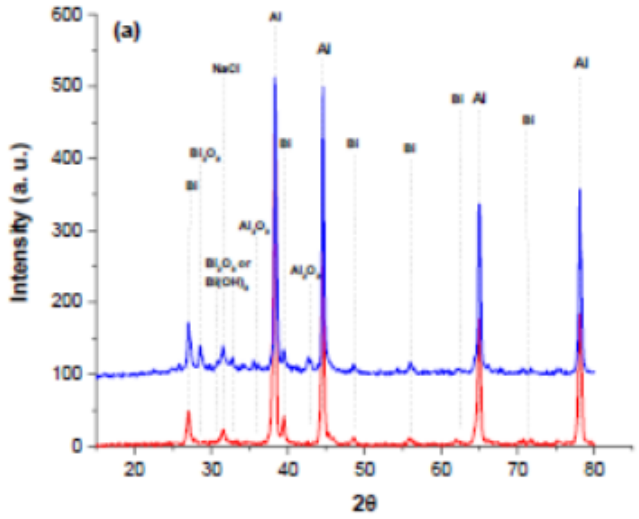

Figure 3.14: XRD patterns of composite powder (red line) and tablet (blue line).

3.6.2. SEM/EDS Analysis

The composite powder's micro-morphology both pre and post ball-milling is illustrated in figure 3.15. Figure 3.15a reveals the presence of aluminum powders that exhibit a poly-dispersed morphology, which includes large spherical aggregates of approximately 40 μm, along with smaller spherical particles ranging in size from 11 μm to 1.5 μm. Figure 3.15b displays these smaller particles surrounding the larger aggregates. In figure 3.15c, the bismuth powder particles appear to be smaller than those of aluminum. The bismuth powder consists of large spherical aggregates, approximately 45 μm in size, as depicted in figure 3.15c. These aggregates are similar in size to those of aluminum powders and are surrounded by spherical particles that are smaller than the aluminum ones. The diameters of these particles range from 3 μm to 0.3 μm, as illustrated in figures 3.15d and 3.15d'.

The composite, produced after ball milling, consists of flat blocks with varying dimensions around 500 m, as presented in figure 3.15e and figure 3.15e'. The size of these blocks is larger than the original aluminum and bismuth particles. The blocks exhibit a thick lamellar morphology due to the layered packing and agglomeration of thinner lamellas, as shown in figure 3.15f. These findings align with Luo P.'s literature data from the International Journal of Hydrogen Energy, which attributes the formation of large agglomerated blocks in the composite to cold-welding between the Al powders during the initial stages of milling [12] [11]. In particular figure 3.15f shows also the presence of internal microscopic defects that are supposed to favour the hydrolysis process [12]. Micrographs presented in figure 3.15g demonstrate that the composite has been compressed into tablets, resulting in a more organized arrangement of blocks and a significant decrease in the active surface area that is exposed.

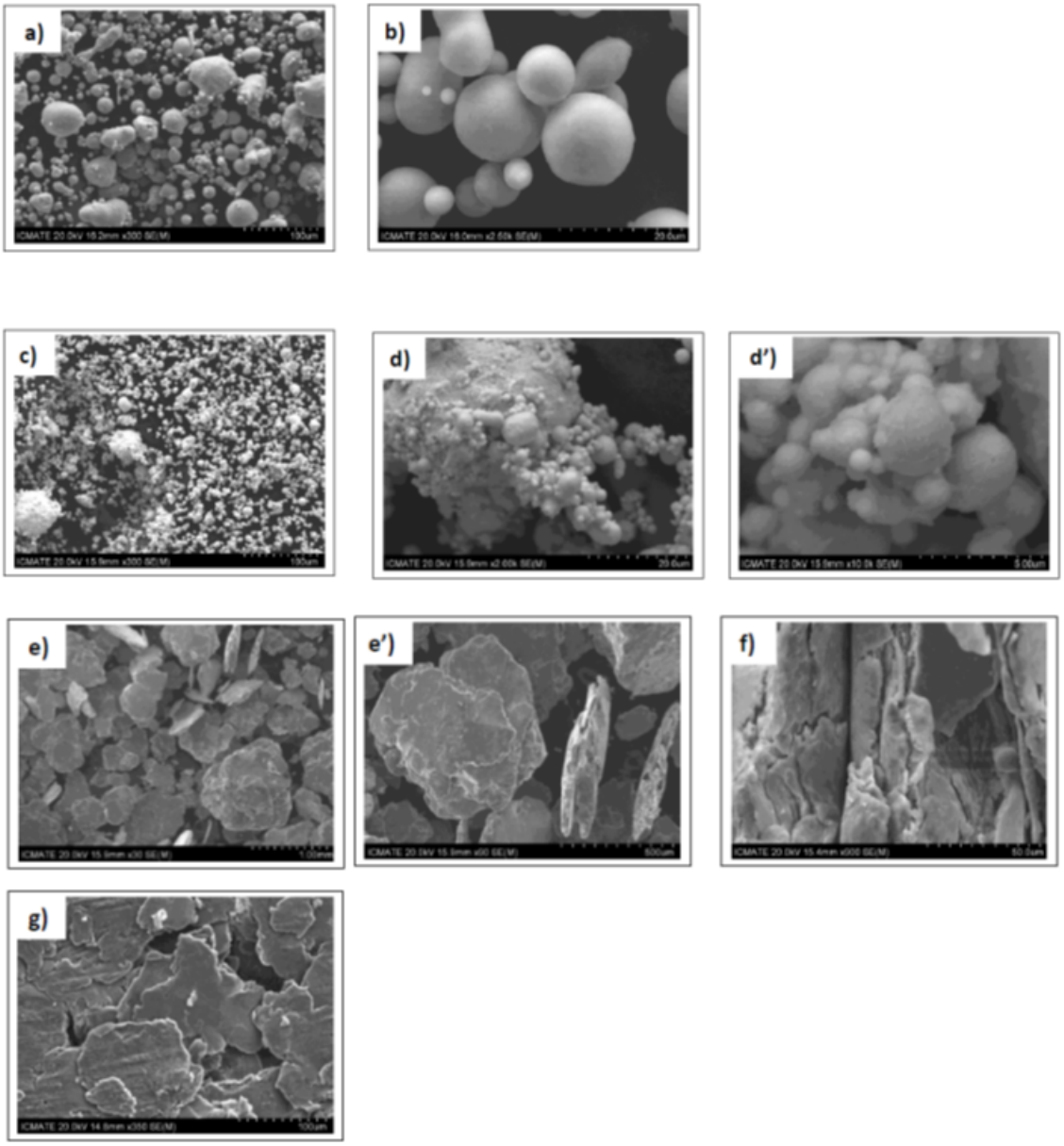

Figure 3.15: SEM images of: a) and b) Al powders; c), d) and d') Bi powders; e) and f) Al/Bi/NaCl composite powders; g) Al/Bi/NaCl composite tablet.

Figure 3.16a shows the EDS mapping and the results of elemental content. One can observe that Bi is present on the Al matrix surface. As the EDS investigation depth is approximately 3 $1mum$, the blank area on the spectrum surface with no detected elements indicates the presence of pits deeper than 3 μm.
The SEM back-scattered images in Figure 3.16b depict the uniform attachment of Bi to the Al matrix without any agglomeration in large clusters. Additionally, the white spots found in the backscattered image cannot be attributed to the existence of bismuth. The uniform spread of Bi indicates the presence of numerous reactive sites, facilitating a sequence of localized galvanic reactions that promote and sustain the entire hydrolysis process [20]. The mass fraction ratio of $Al : Bi$ in the composite (20.49:1; 82.39:4.02) and in the starting material (18:1; 5.4 g:0.3 g) differ insignificantly from each other within the range of experimental error in the EDS analysis. This leads to the supposition that no material in the form of powder is discharged from the stainless steel balls and jar during the milling process affecting the composite.

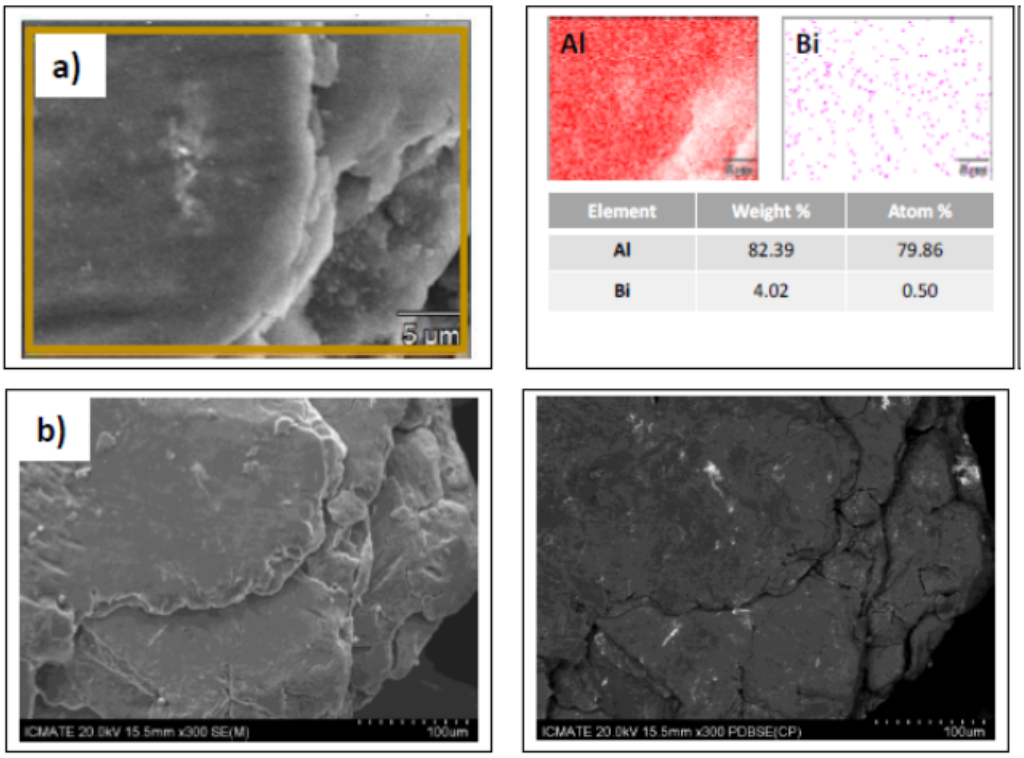

Figure 3.16: Al/Bi/NaCl composite powders: a) EDS mapping; b) SEM and back-scattered images.

4 | Produced Hydrogen Utilization in Space

Hydrogen is increasingly being seen as a pivotal energy carrier for space owing to its superior benefits over other technologies and its eco-friendliness. The aerospace industry first introduced fuel cells with the maiden use of Proton Exchange Membrane (PEM) fuel cell during Gemini missions[3]. When hydrogen is converted into electricity through fuel cells, it can effectively become a power source for propulsion systems in space or aircrafts. This is achieved by utilizing the electricity to fuel a propeller engine.

4.1. Proton Exchange Membrane Fuel Cell

The PEMFC functions as an electrochemical device that transforms hydrogen and oxygen reactants into electrical power, heat, and water, making it an appealing primary power source for human space expeditions, as the hydrogen and oxygen can be used for propulsion systems and the water for crew life-support systems. In this thesis, hydrogen production was achieved through the hydrolysis process discussed in the prior chapter. The PEM fuel cell operates via the following reaction:

$$H_2 + \frac{1}{2}O_2 \longrightarrow H_2O + power \tag{4.1}$$

The production of power through an electrochemical process yields exclusively water, eliminating the presence of harmful byproducts. Essentially, the fuel cell is comprised of two electrodes (the anode and cathode) separated via an electrolyte membrane. The typical operating procedure entails hydrogen being introduced into the fuel cell via the anode, where it ultimately undergoes a reaction with a catalyst to break down into protons and electrons. As this occurs, oxygen is brought in via the cathode. The protons, now possessing a positive charge, move through the porous electrolyte membrane into the cathode. Conversely, the negatively charged electrons exit the cell and generate electric current, which can be utilized to supply electricity to an electric or hybrid-electric

propulsion system. Alternatively, the combination of protons and oxygen in the cathode generates water, allowing the fuel cell to continue generating power as long as a supply of hydrogen and oxygen is available. Furthermore, by stacking individual fuel cells, larger systems can be created, capable of producing even more power. This generated power can then be utilized for a variety of aerospace applications.

4.2. Hydrogen Electric Propulsion

For future orbital space transportation, there is a strong need for high power electric propulsion systems. Ion thrusters are one type of electric propulsion that generate propulsion force by accelerating ions. While ion thrusters have lower strength and acceleration compared to chemical propulsion, they have a higher specific impulse. This means that the same amount of fuel consumed results in more efficient propulsion compared to traditional chemical propulsion, leading to greater flight autonomy and reduced fuel or energy tank requirements. Furthermore, ionic propulsion sources offer a greater specific power advantage. Engines of this nature are best suited for high altitude flights or in vacuum and are employed for spacecraft attitude control utilizing gas that is charged with electrostatic acceleration. Ionic thrusters can be segregated into two groups: electrostatic and electromagnetic. Electrostatic engines employ the Coulomb force to hasten ions, propelling them in the direction of the electric field. On the other hand, electromagnetic engines exploit the Lorentz force to accelerate ions[15].

4.2.1. Magneto Plasma Dynamic and Direct Current Arcjet Thrusters

Magneto Plasma Dynamic (MPD) and Direct Current arcjet (DC) propulsion systems utilizing hydrogen as a propellant show great potential for the mission thanks to their adaptability to high power operation and impressive performance. Their performance is notably heightened when hydrogen is utilized as a propellant. As DC arcjets boost the propellant aerodynamically through the nozzle, those with a smaller molecular weight are preferable for maximizing performance. For hydrogen arcjets, a specific impulse of 1000 to 2000 seconds and an efficiency of 30 to 50% can be reached, compared to an impressive specific impulse of 10,000 seconds achievable with hydrogen MPD thrusters [9].

4.3. Resistojet on Hydrogen Propellant

Hydrogen can be utilized as propellant to power resistojet propulsors. Such a propulsor would operate at a resistor outlet temperature of 2000 K and achieve a specific impulse

of 800 s with a 94.3% specific impulse efficiency. Resistojets are the most commonly used electric propulsion systems, often employed for satellite attitude control and other small-scale maneuvers. This motor operates by heating a non-reactive fluid via electrical current flowing through a resistor made of a hot, glowing filament, with the expanded gas expelled through a nozzle. Boosting heating power at a fixed thrust level raises specific impulse by raising gas temperature through increased specific power. However, higher specific power lowers efficiency due to increased heat losses connected to higher heat exchanger temperature [14].

5 | Conclusions and future developments

The focus of this thesis was to investigate the potential of utilizing the hydrolysis reaction between water and aluminum or magnesium for hydrogen production, which can then be utilized for propulsion purposes. This method holds significance as the produced hydrogen can be directly applied in fuel cells to generate power, or in propulsion systems, particularly in electric thrusters used in space. Moreover, utilizing the hydrogen produced eliminates safety concerns related to its explosive nature or flammability and related to its extremely low density. The focus of the work was centered on attempting to achieve a high yield of hydrogen production through the hydrolysis of water using aluminum and magnesium. Various formulations of powders were tested to determine the optimal efficiency. To prepare the metal powders for the reaction, they were mechanically activated to eliminate the protective oxide layer that forms upon contact with air. The mechanical milling process also involved the addition of other substances, such as $NaCl$, which serves as a means of removing the metal's oxide layer and decreasing particle size due to its brittle nature. Other enhancements, including the infusion of substances like Bi or C, were also employed to improve the reaction. In order to test hydrogen production, the powder was not directly inserted into water. Instead, it was compressed into tablets using a mold. The hydrolysis reaction was then used to test the production of hydrogen by displacing water. This was accomplished using an experimental setup consisting of a reactor filled with water that was connected to a glass reading column. The tablet was placed in the reactor, and when it reacted, any hydrogen produced moved through the connection tube to the reading column. Due to its lower density, the hydrogen occupied the upper part of the column while pushing the water downwards. This allowed for the measurement of the amount of hydrogen produced, with readings taken at specific time intervals to determine the rate of hydrogen production. Three formulations were tested, with two containing only aluminum and one containing both aluminum and magnesium. Among them, only the formulation consisting of $Al - Bi - NaCl$ achieved nearly 100% efficiency and showed faster hydrogen production, generating 90 % of the total hydrogen in just 6

minutes and 30 seconds. The other two formulations displayed a lower efficiency and a different production trend, as they steadily produced hydrogen but at a slower rate.

The study has demonstrated how the process of hydrolyzing water using metal elements can be utilized to generate hydrogen in an eco-friendly and secure manner. Based on this assertion, a set of theoretical subsequent measures is outlined below:

- A study aimed to investigate the efficacy of varying additives materials or percentages in aluminum and magnesium-based powder formulations to achieve improved reaction efficiencies.
- A study which involves altering the temperature conditions of the reaction, such as increasing the temperature to higher levels as it has been observed to optimize the reaction.
- A study which involves altering the environmental factors that affect the reaction process, such as testing the efficiency of aluminum reaction in alkaline solutions or magnesium reaction in acidic solutions.

To summarize, extensive research is required to identify alternative formulations, aside from the $Al-Bi-NaCl$ composition, that can yield highly effective reactions. Additionally, identifying the most effective additives to enhance this reaction in water is crucial. However, despite the challenges, global interest in this innovative technology is growing, and some experiments conducted in this thesis have yielded promising results.

References

[1] B. Alinejad and K. Mahmoodi. A novel method for generating hydrogen by hydrolysis of highly activated aluminum nanoparticles in pure water. *International Journal of Hydrogen Energy 34*, pages 7934–7938, 2009.

[2] A. Bolt and I.Dincer. Experimental study of hydrogen production process with aluminum and water. *International Journal of Hydrogen Energy 45*, pages 14232–14244, 2020.

[3] J. Brey, D. Munoz, V. Mesa, and T. Guerrero. Use of fuell cells and electrolyzers in space applications: from energy storage to propulsion/deorbitation. *E3S Web of Conferences 16*, 2016.

[4] K. Eom, J. Kwon, M. Kim, and H. S. Kwon. Design of al-fe alloys for fast on board hydrogen production from hydrolysis. *Journal of Materials Chemistry*, 2011.

[5] M. Grosjean, M. Zidoune, L. Roué, and J.Y.Huot. Hydrogen production via hydrolysis reaction from ball-milled mg based materials. *International Journal of Hydrogen Energy 31*, pages 109–119, 2005.

[6] X. Huang, C. Lv, Y. Wang, H. Shen, D. Chen, and Y. Huang. Hydrogen generation from hydrolysis of aluminum/graphite composites with a core-shell structure. *International Journal of Hydrogen Energy 37*, pages 7457–7463, 2012.

[7] A. Iljukhina, A. Iljukhin, and E. Shkolnikov. Hydrogen generation from water by means of activated aluminum. *International Journal of Hydrogen Energy 37*, pages 16382–16387, 2012.

[8] A. Irankhah, S. Mohsen, S. Fattahi, and M. Salem. Hydrogen generation using activated aluminum/water reaction. *International Journal of Hydrogen Energy 43*, pages 15739–15748, 2018.

[9] K. Kinefuchi, K. Okita, H. Kuninaka, D. Nakata, T. Suzuki, and H. Tahara. Preliminary study of high power hydrogen electric propulsion for the space exploration. *50th AIAA/ASME/SAE/ASEE Joint Propulsion Conference*, 2014.

[10] Y. Liu, X. Liu, X. Chen, S. Yang, and C. Wang. Hydrogen generation from hydrolysis of activate al-bi, al-sn powders prepared by gas athomization method. *International Journal of Hydrogen Energy 42*, pages 10943–10951, 2017.

[11] P. Luo. *J. All. Comp.*, 2019.

[12] P. Luo. *International Journal of Hydrogen Energy 45*, pages 13139–13148, 2020.

[13] D. Marotto. Hydrogen generation by water hydrolysis to support pem fuel cells technology. *Master Thesis, Politecnico di Milano*, 2021.

[14] C. Mijake and F. McKevitt. Performance characterizations tests of a 1-kw resistojet using hydrogen, nitrogen and ammonia as propellants. *21st Joint Propulsion Conference*, 1985.

[15] R. Petrescu, A. Machin, K. Fontanez, J. Arango, F. Marquez, and F. Petrescu. Hydrogen for aircraft power and propulsion. *International Journal of Hydrogen Energy 45*, pages 20740–20764, 2020.

[16] C. Porciùncula, N. Marcilio, I. Tessaro, and M. Gerchmann. Production of hydrogen in the reaction between aluminum and water in the presence of naoh and koh. *Brazilian Journal of Chemical Engineering*, 29:337–348, 2011.

[17] S. Razavi-Tousi and J. Szpunar. Effect of addition of water-soluble salts on the hydrogen generation of aluminum in reaction with hot water. *Journal of Alloys and Compounds 679*, pages 364–374, 2016.

[18] C. Wang, Y. Chou, and C. Yen. Hydrogen generation from aluminum and aluminum alloys powder. *Procedia Engineering 36*, pages 105–113, 2011.

[19] F. Xiao, R. Yang, and Z. Liu. Active aluminum composites and their hydrogen generation via hydrolysis reaction: A review. *International Journal of Hydrogen Energy 47*, pages 365–386, 2021.

[20] W. Yang, T. Zhang, J. Zhou, W. Shi, J. Liu, and K. Cen. Experimental study on the effect of low melting point metal additives on hydrogen production in the aluminum-water reaction. *Energy 88*, pages 537–543, 2015.

[21] Y. Yavor, S. Goroshin, J. Bergthorson, and D. Frost. Comparative reactivity of industrial metal powders with water for hydrogen production. *International Journal of Hydrogen Energy 40*, pages 1026–1036, 2014.

[22] Y. Yia, J. Schen, H. Meng, Y. Dong, Y. Chai, and N. Wang. Hydrogen generation

using a ball-milled al/ni/nacl mixture. *Journal of Alloys and Compounds 588*, pages 259–264, 2013.

[23] H. Zou, S. Chen, Z. Zhao, and W. Lin. Hydrogen production by hydrolysis of aluminum. *Journal of Alloys and Compounds 578*, pages 380–384, 2013.

A | Appendix A

A.1. Powders

Formulation	Al(90)	Bi(5)	NaCl (5)
Initial mass sample [mg]	0.500	0.506	0.519
H_2 volume	604	620	620
Ambient temperature [°]	24	24	24
Pressure at sea level [mbar]	1005	1005	1005

Table A.1: Powder Al-Bi-NaCl Data.

Formulation	Al(90)	C(5)	NaCl (5)
Initial mass sample [mg]	0.501	0.489	0.503
H_2 volume	45	42	52
Ambient temperature [°]	22	22	22
Pressure at sea level [mbar]	1003	1012	1012

Table A.2: Powder Al-C-NaCl Data.

Formulation	Mg+Al(90)	Bi(5)	NaCl (5)
Initial mass sample [mg]	0.501	0.502	0.500
H_2 volume	70	67	66
Ambient temperature [°]	20.5	22	23.5
Pressure at sea level [mbar]	1003	1003	1003

Table A.3: Powder Mg-Al-Bi-NaCl Data.

Ringraziamenti

Il primo ringraziamento va al mio relatore, il professor Galfetti, per avermi dato la possibilità di scegliere questa tesi e di poter svolgere attività sperimentali in laboratorio. Ringrazio anche Stefano e Alessandro per tutti i dubbi che mi hanno aiutato a risolvere senza i quali non sarei riuscita a condurre la mia campagna sperimentale. Ringrazio Alberto, per la disponibilità nell'aiutarmi in ogni problema di natura tecnica. Inoltre senza di lui non avrei avuto un apparato da poter utilizzare per condurre i miei esperimenti. Ringrazio tutta la mia famiglia per avermi sempre sostenuto durante il mio percorso universitario e per avermi sempre supportato in tutte le mie scelte nonostante qualche sacrificio da fare. Ringrazio Giorgia, che nonostante la lontananza e i vari impegni so che è sempre presente e sempre disponibile a supportarmi. Ringrazio Martina, l'amica più storica che io abbia, per avermi fatto compagnia nei week end in patria e per non avermi fatto sentire sola durante le difficoltà universitarie. Ringrazio Nicole, quell'amica su cui posso contare sempre e soprattutto se voglio cercare un'avventura, a volte anche fin troppo estrema. Ringrazio tutti i miei amici dell'università, nonchè compagni di innumerevoli avventure: Andrea, Chiara, Francesca, Ludovica, Mirko, Orso e Pedro per aver svolto questo percorso tutti insieme. Mi hanno permesso di rendere piacevoli e pieni di fantastiche esperienze questi anni, dandomi inoltre molti ricordi oltre a quelli universitari, come grigliate, viaggi fatti insieme e soprattutto tanti aperitivi. Infine ringrazio tutte le persone che ho incontrato lungo il mio percorso di studi e che hanno contribuito a renderlo così piacevole.